



Department of Chemistry and Biomolecular Sciences

**Effect of carbon source on the
glycosylation pathway of *Trichoderma*
reesei RUT-C30**

Chris Ashwood

Bachelor of Forensic Science

10th of October, 2014

A dissertation submitted in partial fulfilment of the Master of Research degree

Table of Contents

Declaration	iii
Acknowledgements	iv
Abstract	v
Abbreviations and symbol nomenclature	vi
Chapter 1 – Introduction	1
1.1 The fungus <i>Trichoderma reesei</i> RUT-C30: a protein production machine.	1
1.1.1 History of the strain	1
1.1.2 Protein glycosylation in <i>Trichoderma reesei</i>	2
1.2 Metabolomics	6
1.2.1 Metabolomics in cellular physiology	7
1.2.2 Targeted and untargeted metabolomics.....	7
1.2.3 Nucleotide-sugars.....	8
1.2.4 ATP, ADP and AMP nucleotides.....	11
1.3 Methods for metabolite analysis.....	12
1.3.1 Microbial cell culture	13
1.3.2 Cell quenching and metabolite extraction	14
1.3.3 Metabolite separation and analysis	15
1.4 Evaluation of protein <i>N</i> - and <i>O</i> -glycosylation.....	16
1.5 Research aims.....	17
Chapter 2 - Materials and Methods	18
2.1 Chemicals, proteins and other materials.....	18
2.2 Fungal strain	18
2.3 Biolog assay	18
2.4 Liquid cultivation in shake flasks	19
2.5 Monitoring of culture pH and mycelial growth	19
2.6 CBHI activity.....	20
2.7 Protein concentration.....	20
2.8 Extraction of nucleotides and nucleotide sugars	21
2.8.1 Quenching fungal cells and extraction of polar metabolites	21
2.8.2 Capillary electrophoresis with diode array detection	21
2.8.3 Analysis of the ATP standard using mass spectrometry.....	22
2.9 Sodium dodecyl sulphate polyacrylamide gel electrophoresis (SDS-PAGE) and protein identification by mass spectrometry.....	22
2.10 <i>N</i> -glycan and <i>O</i> -glycan analysis of secreted proteins.....	23

2.10.1 Protein immobilisation and <i>N</i> -glycan/ <i>O</i> -glycan release	23
2.10.2 Mass spectrometric analysis of released glycans	24
2.10.3 Data Analysis	25
Chapter 3 Results	26
3.1 Physiological studies	26
3.1.1 Biolog assay for carbon utilisation	26
3.1.2 Mycelial growth and pH of shake flask cultures with glucose or lactose as sole carbon source.....	27
3.1.3 Protein secretion and CBHI activity in the culture supernatants.....	29
3.2 Analysis of nucleotides and nucleotide sugars	30
3.2.1 CE-UV method development for metabolite analysis.....	30
3.2.2 Comparison of nucleotide–sugar and nucleotide pools in RUT-C30 grown on glucose and lactose	32
3.3 <i>N</i> -glycan and <i>O</i> -glycan analysis of secreted proteins	33
Chapter 4 Discussion	41
4.1 The value of Biolog assays for determining carbon source utilisation of <i>T. reesei</i>	41
4.2 Growth phases of <i>T. reesei</i> under different carbon sources.....	42
4.3 Secreted protein concentration and CBHI activity show similar but not identical trends over the cultivation period.....	44
4.4 Analysis of nucleotides and nucleotide sugars	44
4.4.1 Preparation of samples for CE-UV analysis.....	44
4.4.2 Nucleotide and nucleotide sugar analysis.....	45
4.5 <i>N</i> -glycan and <i>O</i> -glycan profiles of secreted protein.....	47
4.5.1 The relative abundance of <i>N</i> -glycans in glucose and lactose cultures.....	47
4.5.2 Phosphorylation of <i>N</i> -glycans	48
4.5.3 The identification of extended <i>O</i> -glycan compositions	49
4.5.4 Identification of HexA in <i>O</i> -glycans of <i>T. reesei</i>	49
4.5.5 Role of negatively charged glycans in <i>T. reesei</i> and yeast	50
Chapter 5 Summary and future directions	51
Chapter 6 References.....	a
Chapter 7 Supplementary Material	i
7.1 Biolog.....	i
7.2 Capillary electrophoresis.....	k
7.3 <i>N</i> -glycan and <i>O</i> -glycan MS/MS structures table	m
7.4 Annotated MS/MS of <i>O</i> -glycans.....	o
7.5 Identification of CBHI as a major constituent of total secreted protein.....	r

Declaration

This thesis is a presentation of my original research work carried out as part of the Master of Research program at Macquarie University. Wherever contributions of others are involved, every effort is made to indicate this clearly, with due reference to the literature, and acknowledgement of personal assistance or advice.

The thesis is formatted according to Master of Research guidelines and the journal *Glycobiology*.

Chris Ashwood

Acknowledgements

This thesis would look very different and very bare without the help of those I have encountered throughout my nine months of research at Macquarie University. I would like to thank the following groups and people for their contribution to my thesis and my development as a scientist:

Glyco@MQ: My supervisor Nicki Packer for taking me on as a student 3 months in, as well as the continued support and guidance for all work I performed and keeping it all about the story. Jodie, for her assistance with many aspects of thesis including training me on nucleotide sugar analysis with CE-UV, N-/O-glycan release and data analysis. Robyn, for her knowledge, editorial experience and support. Liisa, for her lab management and technical assistance. Arun, for his technical knowledge, especially mass spectrometry. The rest of the group (which I wouldn't be able to fit in a page) for their assistance

Nevalainen group: Helena Nevalainen, for support and assistance, I appreciate your investment in me. Junior and Angela, for training me up in *Trichoderma*. The rest of the group for their assistance throughout the year and listening to me present, as well as their valuable suggestions.

Australian Proteome Analysis Facility (APAF): Dylan for his assistance with peptide analysis for protein identification. Georgina for her assistance with monosaccharide analysis

Everyone else: Ani, for her assistance with Biolog. David H. and Steph for office discussions. Paul, for his mentoring, discussions about anything and maintaining my sanity. Bridget, for all her MRes administration. This thesis wouldn't exist without her. Heather and my family, for supporting me and also keeping me sane.

Abstract


Trichoderma reesei has been of industrial interest for several decades for the production of cellulases, resulting in the development of hypercellulolytic strains such as RUT-C30. High protein production and secretion, and eukaryotic glycosylation machinery, make *T. reesei* RUT-C30 a suitable expression host for recombinant proteins. The glycosylation of secreted proteins of RUT-C30 is known to vary depending on culture nutrients. However, the impact of media on the intracellular precursors of glycosylation and on the secreted protein glycosylation has received little attention, and techniques for their analysis in fungi are lacking.

This study investigated the effect of carbon source on nucleotide sugars of RUT-C30, important precursors of glycosylation. Methods were developed to extract and analyse these metabolites from mycelia grown on glucose or lactose. In parallel, the glycosylation profile of secreted protein was monitored. Differences were found in the abundance of nucleotide sugars depending on carbon source, not directly reflected in secreted protein glycosylation. In addition, previously uncharacterised *O*-glycan structures on the total secreted protein were identified. The work provides insight into the effect of carbon sources on the glycosylation and protein secretion pathways in *Trichoderma reesei* RUT-C30, with the long term aim of regulating the production of recombinant secreted proteins.

Abbreviations and symbol nomenclature

ADP	Adenosine diphosphate	HPLC	High performance liquid chromatography
AEC	Adenylate energy charge	ICC	Ion charge control
AMP	Adenosine monophosphate	KEGG	Kyoto Encyclopaedia of Genes and Genomes
Asn	Asparagine	LC	Liquid chromatography
ATP	Adenosine triphosphate	LTQ-XL	Linear ion trap
BSA	Bovine serum albumin	Man	Mannose
CBHI	Cellobiohydrolase I	MS	Mass spectrometry
CBHII	Cellobiohydrolase II	MS/MS	Tandem mass spectrometry
CDP	Cytidine diphosphate	NeuAc	<i>N</i> -acetyl-neuraminic acid
CE	Capillary electrophoresis	NMR	Nuclear magnetic resonance
CHO	Chinese hamster ovary	NTG	Nitrosoguanidine
CMP	Cytidine monophosphate	P	Phosphate
CTP	Cytidine triphosphate	PAGE	Polyacrylamide gel electrophoresis
EGI	Endoglucanase I	PDA	Potato dextrose agar
EGII	Endoglucanase II	PGC	Porous graphitised carbon
EGV	Endoglucanase V	PIPES	Piperazine- <i>N</i> - <i>N'</i> -bis
ER	Endoplasmic reticulum	PNGase-F	Peptide- <i>N</i> -glycosidase F
ESI	Electrospray ionisation	PVDF	Polyvinylidene fluoride
FF	Filamentous fungi	SDS	Sodium dodecyl sulphate
GalNAc	<i>N</i> -acetyl-galactosamine	Ser	Serine
GC	Gas chromatography	Thr	Threonine
GMP	Guanosine monophosphate	UDP	Uridine diphosphate
GTP	Guanosine triphosphate	UMP	Uridine monophosphate
Hex	Hexose	UTP	Uridine triphosphate
HexA	Hexuronic acid	UV	Ultraviolet detection

Glycan analysis symbol nomenclature

	Glucose		<i>N</i> -acetyl glucosamine
	Hexuronic acid		Phosphate
	Mannose		Reduced end

Chapter 1 – Introduction

1.1 The fungus *Trichoderma reesei* RUT-C30: a protein production machine.

1.1.1 History of the strain

The filamentous fungus *Trichoderma reesei* is an industrially important protein secretor that has earned the nickname of “the highly productive black box”. Despite the use of *T. reesei* in industry, the exact reason for the high protein secretion has not yet been determined[1]. The wild-type *T. reesei*, QM6a, was first isolated from a cotton canvas in the Solomon Islands during World War II[2] and was identified as a strain of interest due to its high cellulase production[3]. From here, in depth research into QM6a began, investigating the application of this fungal species in alternate fuel production, specifically bioethanol. As *T. reesei* is a high producer of extracellular cellulase, cellulose-rich biomass can be broken down to form glucose. The glucose can then be fermented by a suitable microorganism, such as yeast, to finish the conversion of cellulose-rich biomass into ethanol[1].

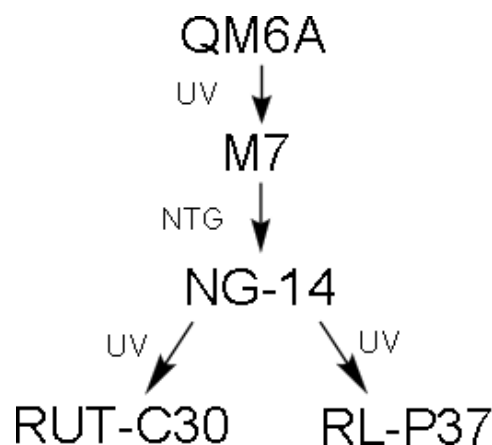


Figure 1. Pedigree of high protein secretion *T. reesei* stains originating from wild-type isolate QM6a with mutations introduced by UV-light (UV) or nitrosoguanidine (NTG). Other strains of the pedigree, including M7, NG-14 and RL-P37, are intermediate or end point mutants in the mutagenesis program. Figure adapted from Seidl *et al.* and updated using information from Peterson *et al* [1,4].

Spurred on by the interest in alternate fuels, high cellulase producing mutants of QM6a were developed by several research groups around the world. One of the earliest successful mutagenesis programs was performed by U.S. Army Natick laboratories[5,6], utilising

mutagenesis by ultraviolet light (UV) and *N*-nitroguanidine (NTG) whilst screening for catabolite derepression by resistance to 2-deoxyglucose. The pedigree of RUT-C30, one of the most promising isolates, is shown in figure 1[1].

When cultured in a cellulase-inducing medium, over 90% of the total proteins secreted by *T. reesei* RUT-C30 are hydrolytic enzymes, predominantly cellulases[7,8]. The five major secreted hydrolases are cellobiohydrolase I and II (CBHI and CBHII), and endoglucanase I, II and V (EGI, EGII and EGV) (Table 1). The main cellulase CBHI is under the control of a strong promoter, inducible by cellulose or disaccharides such as cellobiose, sophorose or lactose, and makes up 50-60% of all secreted protein under inducing conditions. Expression of CBHI in the wild-type QM6a is further characterised by glucose-repression, but a mutation in the RUT-C30 strain enables CBHI production at low levels with glucose as sole carbon source; furthermore, RUT-C30 thus exhibits enhanced CBHI production upon introduction of inducers such as cellulose or lactose, since repression does not occur from glucose produced as an end-product of cellulase activity[9,10].

The RUT-C30 strain has been of industrial and academic interest for cellulase production and as a host for the production of recombinant proteins, often by utilising the strong *cbh1* promoter to drive recombinant gene expression[7]. The use of *T. reesei* as a recombinant protein production organism therefore features high extracellular protein production and secretion, together with eukaryotic glycosylation machinery, potentially making it a more suitable host than other common expression hosts such as *Escherichia coli* which lacks protein secretion and glycosylation[11].

1.1.2 Protein glycosylation in *Trichoderma reesei*

Post-translational modifications are the final preparation steps for protein functionality, involving many processes including folding, assembly, glycosylation and proteolytic cleavage. Protein glycosylation is also important in the function and secretion of proteins and to protect against degradation [12]. Glycoproteins can possess two major classes of glycans: *N*-glycans and *O*-glycans. Each glycan type is bound to different amino acids, with *N*-glycans attached to a nitrogen atom of asparagine residues (Asn) and *O*-glycans attached to an oxygen atom of either serine (Ser) or threonine (Thr) residues[13].

Investigations into glycosylation of proteins in *T. reesei* began over twenty years ago as the activity, stability and secretion of glycoproteins can be modified depending on the

glycosylation profile[14–16]. These studies concentrated on the glycosylation pathways[17] as well as analysis of the nature of sugar groups attached to secreted proteins[14,18–20]. Analysis of the *N*-glycosylation of the secreted hydrolases (Table 1), including CBHI, of RUT-C30 resulted in the identification of glycosylation profiles different to that of human glycoproteins. In particular, the fungal *N*-linked glycans consist mainly of mannose and *N*-acetyl glucosamine (high-mannose glycans) and lack the complex structures containing galactose, fucose or sialic acid that are characteristic of the human *N*-linked glycans[21]. Contrasting this is yeast, a model organism of the fungal kingdom, features highly processed, larger high mannose glycans which are therefore less human compared to those produced by *T. reesei* RUT-C30[22].

Table 1 - Properties of cellulase enzymes secreted by *T. reesei*. Adapted from Edwards, M[23].

Cellulase enzyme	Proportion of total secreted protein (%)	Experimentally verified <i>N</i> -glycosylation Sites	Molecular Weight (kDa)	Reference
CBHI	50-60	Asn 45 Asn 270 Asn 384	59-68	[24] [25]
CBHII	15-18	Asn 289 Asn 310	50-58	[26] [25]
EGI	12-15	Asn 56 Asn 182	50-55	[27] [25]
EGII	9-11	Asn 103	48	[28] [25]
EGV	0-3	Asn 182	23	[28] [25]

The RUT-C30 strain of *T. reesei* is known to have a slightly different *N*-linked glycosylation profile than the wild type QM6a due to the mutation of one of the intracellular glycosidases (glucosidase II) involved in the glycosylation pathway in the endoplasmic reticulum (ER). As a result, high mannose (Man) *N*-glycans on CBHI have been found to feature a terminal glucose (Glc) which is normally removed in the wild-type strain before entering the secretory pathway. It has been hypothesised that this mutation may be associated with the selection for glucose catabolite repression by RUT-C30 through resistance to the antimetabolite 2-deoxyglucose in the mutagenesis and screening program (Section 1.1), a process that

favoured altered glucose transport and metabolism pathways, and modified glycosylation [17,21].

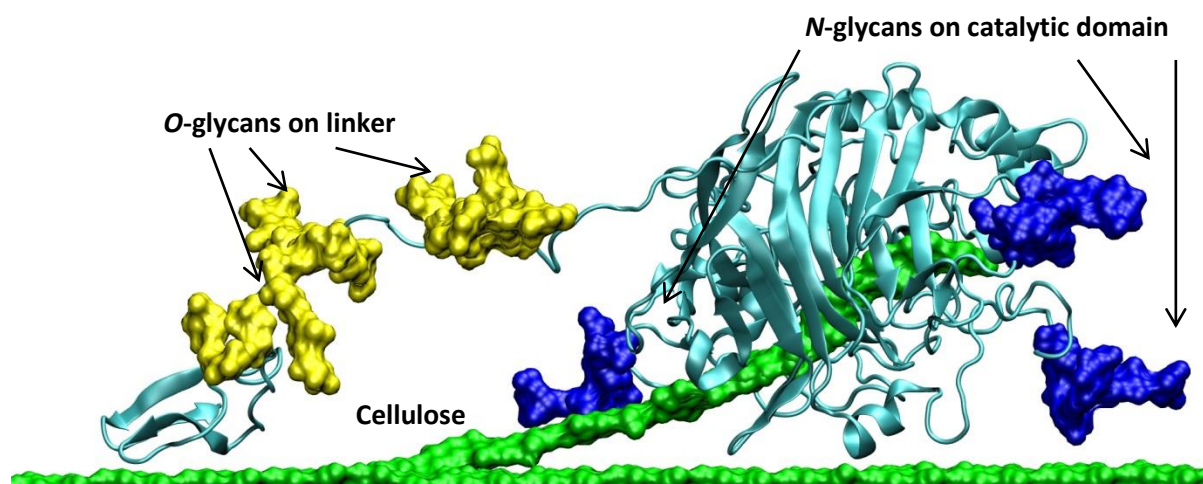


Figure 2. Protein structure of CBH1 bound to cellulose. *N*-glycosylation sites (Asn45, Asn270 and Asn385) highlighted in blue and several *O*-glycosylation sites of the linker region highlighted in yellow.

The *N*-glycosylation of CBHI from *Trichoderma reesei* RUT-C30 varies when grown under different culture conditions [21]. Occupancy of all potential *N*-glycan sites on CBHI (Figure 2) has only been observed when RUT-C30 was grown in minimal medium. The glucose-capped high mannose glycan structure, $\text{GlcMan}_{(7-8)}\text{N-acetyl-glucosamine}_2(\text{GlcNAc}_2)$, and a similar phosphorylated structure, were identified on the three *N*-glycosylation sites of the catalytic domain of CBHI (Figure 2) when grown in minimal medium with lactose as inducer (Table 2). In contrast, cultivation in minimal medium with lactose and calcium carbonate, or complex medium containing corn steep liquor or Solka Floc cellulose, resulted in different *N*-glycosylation profiles, which included single GlcNAc residues on at least two of the three *N*-linked sites and high mannose glycans without glucose caps and no phosphorylation at Asn 270 (Table 2)[21].

The different glycosylation profiles were partly attributed to differences in the pH fluctuations of the culture media during cultivation, which affected the activity of a secreted Endo H-like glycosidase. When grown in the complex culture medium the pH remained relatively stable at 5 - 7, the optimal range for Endo H activity, resulting in cleavage of the *N*-linked glycans leaving only the reducing end GlcNAc attached to the protein. In contrast,

growth in minimal medium resulted in a natural acidification of the culture, secretion of proteases and an inhibition of the extracellular glycosidase activity[17].

In addition to the identified changes to the monosaccharide compositions, phosphorylation of mannose was also observed in *N*-glycans. Phosphorylation of glycans has been identified to play key roles in bacterial pathogenesis, human diseases and protein transport[29–31]. Stals et al. found that phosphorylation of mannose only occurred in minimal growth medium with low pH and also in early stages of cultivation in a rich medium[21].

Table 2. Observed *N*-glycosylation of CBHI from *T. reesei* RUT-C30 with varied growth conditions. Adapted from Stals *et al.*[21]. GlcNAc – *N*-acetyl-glucosamine, Man – Mannose, Glc – Glucose and P – phosphate. The pH and *N*-glycan compositions after five days of cultivation are shown.

Growth Conditions	Medium	pH	Main <i>N</i> -glycan compositions	# of <i>N</i> -glycosylated sites
Shake flasks with lactose	Minimal	2.6	GlcMan ₇₋₈ GlcNAc ₂ ManPGlcMan ₇₋₈ GlcNAc ₂	3
	Complex	5.5	Man ₅ GlcNAc ₂ GlcMan ₇₋₈ GlcNAc ₂	0-1
	Minimal + CaCO ₃	7.5	Man ₅₋₆ GlcNAc ₂ GlcMan ₇ GlcNAc ₂	1-3
Fed-batch fermentation with glucose and cellulose (Solka Floc)	Complex	4.1	ManPGlcMan ₇₋₈ GlcNAc ₂ GlcMan ₇₋₈ GlcNAc ₂	1
	Complex	5.1	GlcMan ₇₋₈ GlcNAc ₂	1
	Complex	5.4	GlcMan ₇₋₈ GlcNAc ₂	1

Despite speculations by Stals *et al.*[21], the role of phosphorylated *N*-glycans in *Trichoderma reesei* RUT-C30 has not been fully determined, with phosphorylated glycans appearing in other prominent strains including QM6a and QM9414[20,32]. Another member of the fungal kingdom, *Saccharomyces cerevisiae*, has been studied extensively with mannose phosphorylation of cell wall glycoproteins identified as a cellular stress response to growth phase and environmental conditions[33]. The phosphate and protein contents of the cell wall increased as the growth rate decreased, with early growth phase cell walls containing little mannose bound phosphate in their oligosaccharides but the amount gradually increased during the late-logarithmic and stationary phases of cell growth[34]. The direct role of mannose phosphorylation in fungi has not been determined but one prevailing

hypothesis is that the mannosylphosphorylation changes the overall negative charge of the cell wall, making it more hydrophilic in order to conserve water and protect cells from drought or high-salt stress[33].

O-glycans, another type of protein glycosylation, have been functionally linked to protein secretion, stability and localisation[16,35–37]. To complement the *N*-glycan structures that have been characterised quite thoroughly, *O*-glycan analysis has been performed on the total secreted protein of *T. reesei*, identifying the length, monosaccharide composition and attachment sites of *O*-linked glycans[21,38]. In contrast to the human *O*-linked glycans, which typically have *N*-acetyl galactosamine (GalNAc) as the first monosaccharide attached to the amino acid, *T. reesei* *O*-glycans contain *O*-linked mannose chains[21]. Christiansen *et al.* have performed glycopeptide analysis on purified secreted proteins of *T. reesei* including CBHI, identifying *O*-linked glycans with mannose residues with lengths ranging from one to four subunits[38].

The influence of the environment on the glycosylation of proteins has been studied extensively in mammalian cell lines; protein glycosylation can be influenced by nutrient limitations, metabolic waste accumulation or by the pH of the culture medium[39–41]. The availability of glycosylation precursors may also be affected by nutrient limitation, and has been investigated in chinese hamster ovary (CHO) cell lines as a limiting factor in the glycosylation of recombinant protein[42]. However, to our knowledge, there has been no published research that has investigated the relationship between growth media, the generation of glycosylation precursors, and resulting secreted protein glycosylation profiles in filamentous fungi. Therefore, quantification of nucleotides (as a measure of energy status) and nucleotide sugars (as a measure of glycosylation precursors) in *T. reesei* grown in different carbon source (glucose and lactose) growth media was undertaken for this thesis (Section 1.3) and the effect on protein glycosylation was evaluated (Section 1.4).

1.2 Metabolomics

The metabolome is the entire set of small molecules (less than 1 kDa) that are present in an organism at a certain time. Examples of such metabolites include metabolic intermediates and metabolic products[43]. Analysis of the metabolites involved in a biological system provides a clear representation of a cell phenotype because of the direct role metabolites play, particularly in the regulation of all biological processes[44].

1.2.1 Metabolomics in cellular physiology

Metabolomics can offer a great wealth of data as they include the precursors and end products of all regulation; therefore, metabolomics is a complementary representation of cell phenotype to transcriptomics and proteomics. Additionally, metabolites are highly connected and changes in gene expression and protein levels can be amplified at the metabolite level[45].

To our knowledge, there has been no research into two important metabolite classes within *Trichoderma reesei*: energy currency and precursors for glycan production. These two classes would be expected to play an important role in the cell itself as well as directly in the production and secretion of glycoproteins[46]. Furthermore, by understanding the role culture media plays in the supply of these metabolites, and the subsequent impact on glycosylation, effective strategies can be designed to manipulate the glycosylation pathway towards desired outcomes for endogenous and recombinant protein production by *T. reesei*.

Metabolomics has the potential to greatly increase our understanding of cell processes. However, the metabolome is complex, involving different turnover rates, complex variations in physiochemical properties of metabolites and in their abundance[47]. There are two broad ways of investigating this complexity, either in a broad shotgun approach (non-targeted) or by targeting specific metabolic pathways, as described below.

1.2.2 Targeted and untargeted metabolomics

Targeted or non-targeted metabolomic studies have advantages and disadvantages in each approach (Table 3). A non-targeted approach usually consists of a comprehensive analysis of all measurable analytes in a sample, leading to the generation of a metabolite fingerprint. From here, the multiple signals can be analysed with data processing software resulting in the identification of overall metabolic profile of the samples. Follow up studies that focus on identifying the compounds that change the fingerprint are performed by mass spectrometry (MS) and/or the use of standards for identification and comparison[48].

Targeted metabolomics, the method used in this thesis, focuses on particular analytes of interest, and uses metabolite-specific measurements that accurately and precisely monitor parameters such as relative abundance. The targeted approach allows more sensitive

detection of molecules with low abundance which can be missed if non-targeted metabolomics methods are utilised[49]. The approach of targeted metabolomics also possesses higher throughput than non-targeted methods but fewer metabolites are identified in a single run[50].

Table 3. Comparison of targeted and non-targeted metabolomics. Adapted from Adamski, J and Suhre, K[51].

Feature	Targeted	Non-targeted
Metabolite Coverage	10-100 (dependant on instrument)	300-1200 (depending on sample matrix)
Sample Throughput	1,000/week	100/week
Methods Used	Ultra performance liquid chromatography (UPLC)-MS/MS, LC-MS, Gas Chromatography (GC)-MS/MS	Nuclear magnetic resonance (NMR), LC-MS/MS, GC-MS/MS
Advantages	Metabolite quantification	Global metabolic fingerprint
Disadvantages	Targeted metabolites only	Semi-quantitative, large range of measurement responses
Main Use	Pathway analysis, kinetics studies, diagnostics	Discovery, differences between phenotypes

The two main classes of *T. reesei* metabolites that were the target of this part of the project were the nucleotide sugars (as part of the glycosylation machinery) and nucleotides (as part of the energy currency of the cell). The project aimed to develop methods for effective detection and quantification of these metabolites in *T. reesei* to provide the foundation for further research that could lead to a better understanding of their biological roles in the expression of recombinant and endogenous proteins.

1.2.3 Nucleotide-sugars

1.2.3.1 Structural features and biosynthesis

Nucleotide sugars, illustrated in figure 3, are composed of a nucleotide, two phosphate groups and a monosaccharide. To synthesise *N*-glycans, the modification of

monosaccharides to form nucleotide sugars is required. The monosaccharides are obtained from various sources including degraded complex carbohydrates and intracellular or extracellular (carbon source) sugars [13]. Although *N*-linked glycosylation takes place within the ER and Golgi, monosaccharide activation and conversion into nucleotide sugars takes place mostly in the cytoplasm. Specific transporters for the nucleotide sugars then carry the activated donors into the Golgi[52].

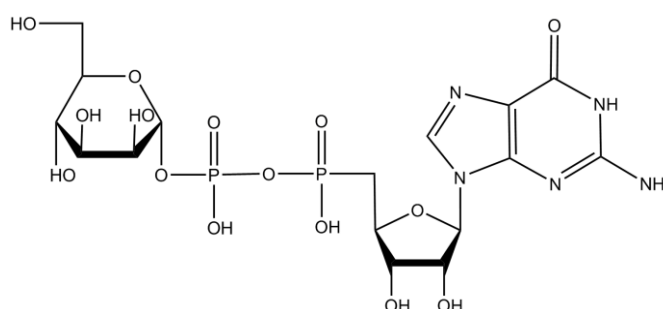


Figure 3 – Typical structure of a typical sugar nucleotide (GDP-Mannose in this case)

To properly synthesise glycans, the monosaccharides must be activated to high-energy donor forms with this process requiring nucleoside triphosphates (such as uridine triphosphate(UTP) or guanosine triphosphate (GTP)) and a glycosyl-1-P, which can be obtained by either kinase interaction or conversion from an alternate glycosyl structure[13].

In *T. reesei*, and almost all forms of life, glucose is the central monosaccharide in carbohydrate metabolism due to its ability to be converted into all other sugars. As part of the glycolysis pathway, extracellular glucose is converted to glucose-6-P and then converted to either fructose-6-P or glucose-1-P by phosphoglucose isomerase[53]. Glucose-1-P is the most common form of a glycosyl donor with the high-energy donor, uridine diphosphate glucose (UDP-Glc), able to be produced upon reaction with UTP. Due to its direct link to glycolysis, the UDP-Glc pool is quite large and can enable synthesis of other glucose-containing molecules such as dolichol-P-glucose, which is essential for the biosynthesis of *N*-glycans[13].

Much like glucose, other monosaccharides such as mannose and fucose can also be used for the biosynthesis of glycans. Both mannose and fucose are activated by GTP allowing phosphorylation of the monosaccharide to form GDP-Man and GDP-Fuc respectively. Uridine diphosphate *N*-acetyl-glucosamine (UDP-GlcNAc) is formed by the *N*-acetylation of

glucosamine-6-P to produce *N*-acetylglucosamine-6-P and then modified to form *N*-acetylglucosamine-1-P. From here, synthesis is the same as other glycosyl donors with the reaction of *N*-acetylglucosamine-1-P with UTP to form UDP-GlcNAc. Whilst these are the most common pathways for the synthesis of these glycosyl donors, several salvage pathways are present leading to a highly interlinked biosynthesis pathway[13].

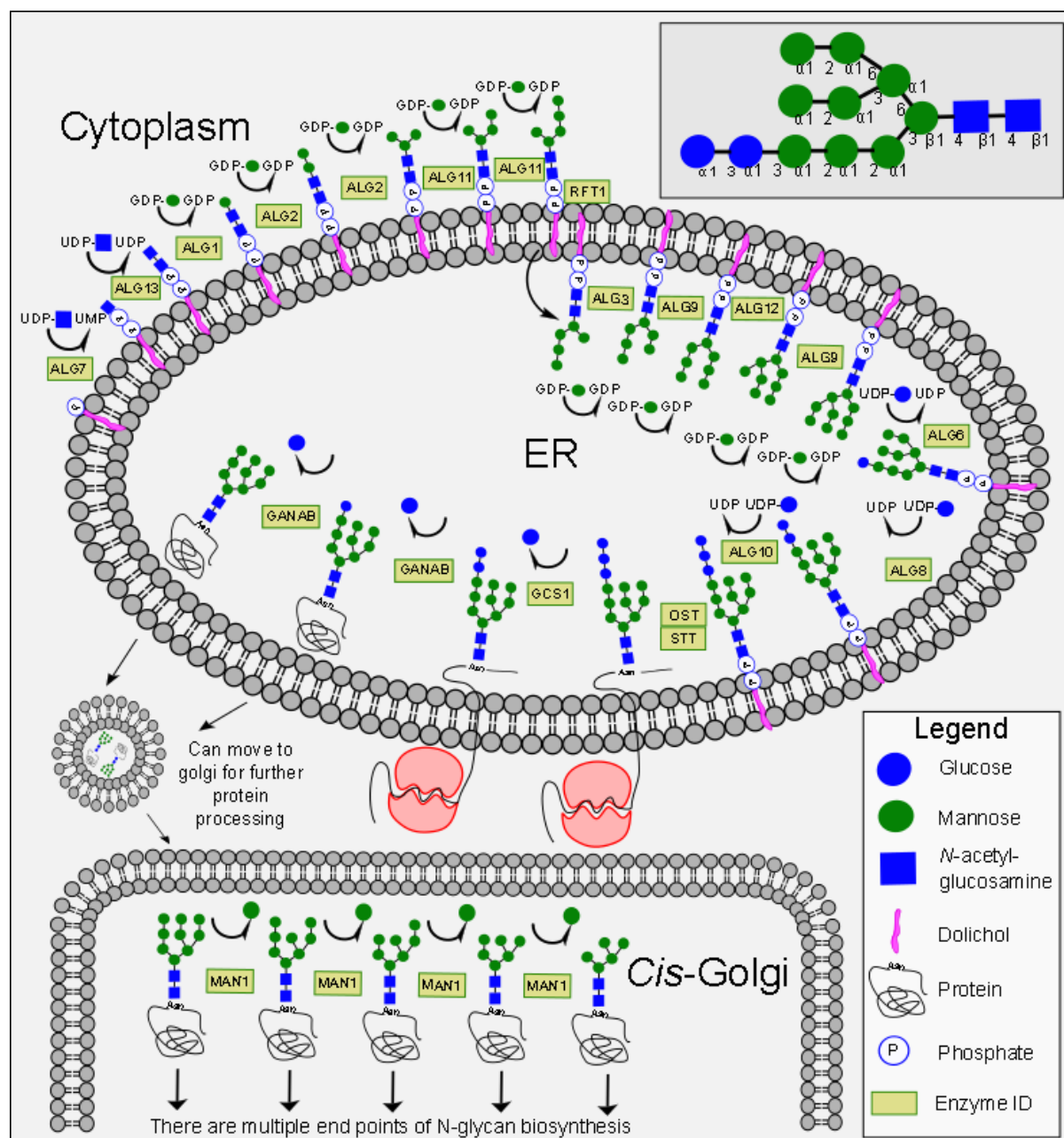


Figure 4 – Predicted *N*-glycan biosynthetic pathway based on genomic and proteomic pathway mapping of the wild-type species, *Trichoderma reesei* QM6a, in KEGG[54]. The RUT-C30 strain is known to have a mutation in glycosidase II (GANAB). Featured inset, the

largest *N*-glycoform observed on secreted RUT-C30 glycoproteins with linkages based on previous research into fungal *N*-glycans[55,56].

The biosynthesis of major classes of glycans in the ER and Golgi compartments in humans has been well characterised. Glycosylation reactions using nucleotide sugars as donors are catalysed by glycosyltransferases, which add monosaccharides one at a time to the glycan chains. Fungal cells have a similar, but truncated biosynthetic pathway in comparison to humans, and produce eukaryotic type high mannose *N*-linked glycans as shown in figure 4[56], but generally not the more complex human-like glycans containing other types of monosaccharide sugars (e.g. galactose, fucose). The sequential nature of glycosylation requires the availability of nucleotide sugars in the ER, controlled through transporter regulation[52,56,57].

In fungi, all nucleotide sugars are synthesised in the cytoplasm and are subsequently moved to the appropriate organelle by specialised nucleotide sugar transporters [58]. All these nucleotide sugar transporters are encoded by specific genes with most transporters specific to one type of nucleotide sugar[52].

1.2.4 ATP, ADP and AMP nucleotides

1.2.4.1 Biological roles of ATP and its derivatives

ATP is the main energy source for the majority of cellular functions. An important part of cellular function is the synthesis of macromolecules and ATP is involved in DNA, RNA and protein synthesis[59]. Since the whole process of glycosylation is influenced by many intracellular factors, including the availability and function of glycan synthesising and modifying enzymes, and precursors such as nucleotide sugars. All of these factors could be influenced by the availability of energy which can be represented by the relative abundance of ATP.

A measure used to represent the metabolic energy state of a cell or organism is called the adenylate energy charge (AEC), defined as $(ATP + 0.5 * ADP) / (AMP + ADP + ATP)$ [60]. A relationship between glycosylation and AEC was proposed in a study that found that a lower AEC in chinese hamster ovary (CHO) cells resulted in a significant reduction in the overall size of a recombinant glycoprotein, which suggested reduced *N*-glycosylation[42]. Whilst the

cells used for this study were mammalian, the initial glycosylation process is the same in filamentous fungi such as *T. reesei*, making it a useful model for comparative purposes.

1.2.4.2 Structural features and biosynthesis

Adenosine-5'-triphosphate (ATP), as seen in figure 5, is comprised of a ribose sugar, an adenine ring and three phosphate groups, both attached to the 1' and 5' carbons of the ribose sugar respectively. ATP is often used for energy transfer in the cell with ATP synthase producing ATP from ADP or AMP by addition of phosphate groups[61]. Despite its many functions, ATP is an unstable molecule which hydrolyses to ADP and inorganic phosphate when it is in equilibrium with water. To stabilise this molecule within the cell, Mg^{2+} binds to the negatively charged phosphate groups[61].

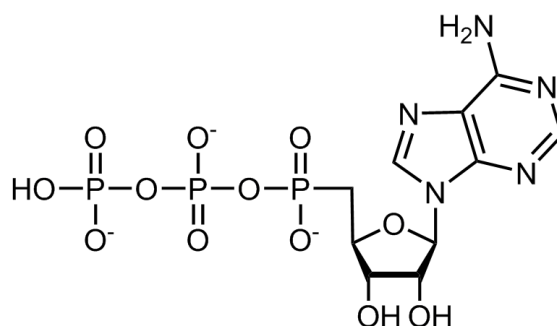


Figure 5 – The chemical structure of ATP

The three high energy phosphate bonds of ATP are the source of the high potential energy of this molecule. The cleavage of a phosphate group from ATP results in the coupling of energy to metabolic reactions and a by-product, a molecule of adenosine diphosphate (ADP)[61]. In a continual cyclic process, ATP can then be reformed by phosphorylation of ADP and adenosine monophosphate (AMP). AMP is one of the many nucleoside monophosphates produced from the breakdown of RNA making it highly involved in cellular metabolism[59].

1.3 Methods for metabolite analysis

Metabolite analysis presents a number of challenges. Firstly, organisms must be cultured in an appropriate medium to enable examination of a metabolite pathway of interest. Secondly, cells must be quenched using ice cold solvents to rapidly arrest any enzymatic activity to minimise associated impact on the metabolome, and in a reproducible manner to

enable comparison of samples. Thereafter, the metabolites must be extracted, separated and analysed using techniques that suit their physiochemical properties and varied abundance[62]. In the following sections, methods suitable for the metabolite analysis of *T. reesei* are described. To our knowledge, there has not been any published method for the analysis of ATP derivatives and nucleotide sugars specifically in *T. reesei*; however, methods used for metabolite analysis in similar organisms are described in section 1.3.3 and their suitability for a fungal system assessed as part of the experimental work of this thesis.

1.3.1 Microbial cell culture

High-throughput screening technologies have been developed to compare the growth of bacterial and fungal strains on a wide variety of media. Results from these analyses can then be utilised in designing appropriate nutrient media for large scale cultivation, depending on the aim of the research exercise. The Biolog phenotype microarray plates have been developed to screen microbial strains for nitrogen or carbon utilisation, with specific compounds. This type of screening allows classification of microbial species based on their signature phenotypes demonstrated through carbon utilisation for example[63–65]. Recently, strains of *Trichoderma reesei* have been screened using carbon source microplates, in order to compare their metabolic activities and for screening their carbon utilisation capacities[66]. These types of studies allow the comparison of similar strains of the same species despite this type of technology initially being developed for screening and characterising phenotypically distinct species[64]. For this thesis, carbon source utilisation of *T. reesei* was monitored using Biolog microarray prior to the more traditional larger scale laboratory cultivation in defined medium using shake flasks.

The laboratory scale cultivation of *T. reesei* has been performed for over thirty years with a minimal medium established by Penttilä et al. that contains the minimum requirements necessary to support the growth of *T. reesei*[27]. This provides a consistent base to which different carbon sources can be added to investigate the effect on the metabolome. Since the expression of the main *T. reesei* secreted cellulase CBHI is controlled by an inducible gene promoter, inducers such as cellulose or lactose are typically included in the liquid culture medium to boost CBHI production. The RUT-C30 strain also produces low amounts of CBHI in the presence of glucose, due to a mutation in a gene (*cre1*) that causes glucose-repression of the *cbh1* promoter in the wild-type[9,10]. Therefore, cultivation of the mutant

strain RUT-C30 on lactose and on glucose (*i.e.* with and without cellulase gene induction), presented two interesting scenarios for targeted metabolite analysis and for the parallel analysis of the glycosylation of the secreted product CBHI (albeit typically lower on glucose) in both growth conditions.

1.3.2 Cell quenching and metabolite extraction

Quenching and extraction methodologies play a huge role in the analysis of metabolites to facilitate an effective snapshot of the cell at the time of sampling. Ideal quenching and extraction protocols should meet certain minimum prerequisites, which include instantly arresting cellular metabolic activity with no significant cell membrane damage. A common workflow involving cell quenching, metabolite extraction and analysis is shown in figure 6[62] and a proposed quenching protocol with no leakage of ATP has been demonstrated with other filamentous fungi species[67].

Quenching and extraction protocols reviewed by Mashego *et al*[62], offer many different techniques that can be applied to filamentous fungi. For the analysis of polar metabolites, a large class of metabolites, Villas-Bôas *et al*[68] compared many extraction and quenching protocols, finding washing and quenching essential for robust cellular metabolite extraction with one procedure involving a methanol quenching step to wash any extracellular compounds from the culture medium whilst ensuring that the temperature of the cells is brought to an appropriate level to inactivate enzymes and thus quench metabolic activity. Following quenching, extraction solvents such as boiling ethanol and chloroform:methanol:water have been used for cell lysis to quickly and effectively break open the fungal cells. These methods reduce the loss of metabolites that would result from other cell lysis techniques through extended sample handling[69].

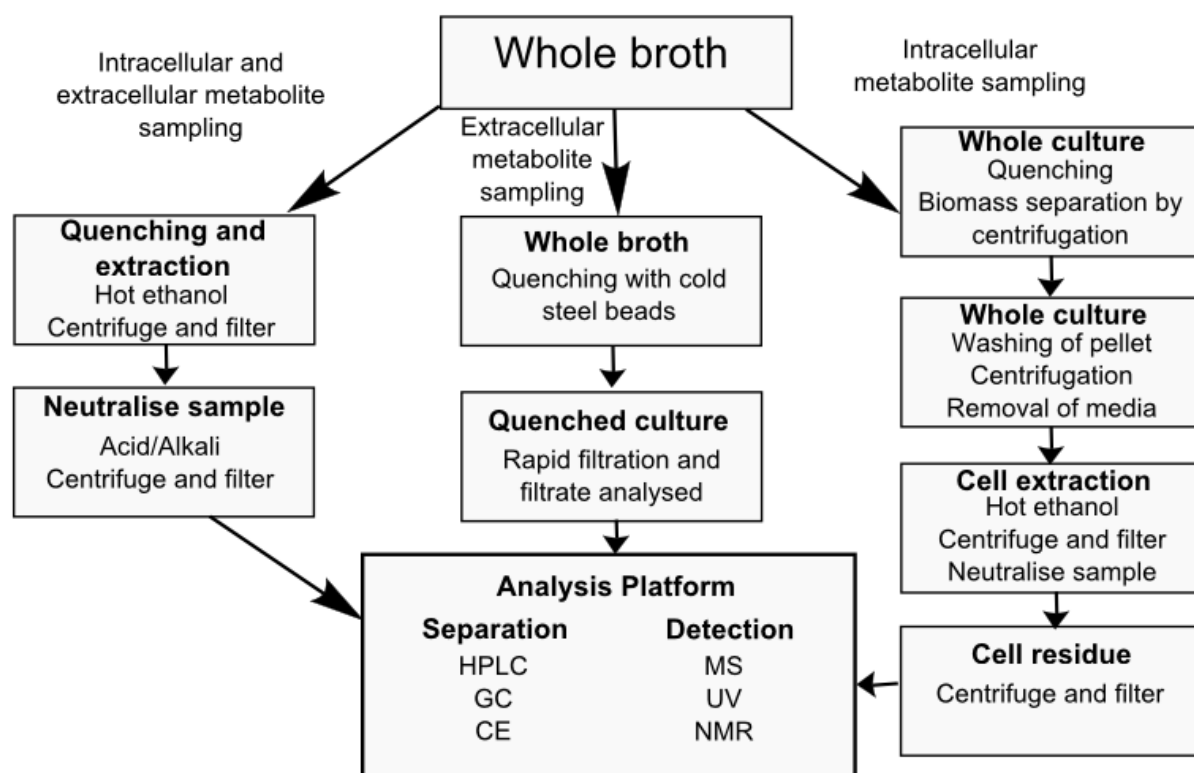


Figure 6. Common sample preparation workflows for metabolite analysis depending on the metabolites of interest. Adapted from Mashego *et al.* [62].

To enhance the sensitivity of the analysis techniques for detection and quantification of nucleotide-sugars and nucleotides, targeted purification of polar metabolites is recommended. This reduces the influence of non-targeted metabolites on analysis which improves consistency between samples with varying cellular metabolite profiles[70]. Following the extraction of polar metabolites, such as nucleotide sugars, samples are ready for separation and analysis with capillary electrophoresis – ultraviolet detection (CE-UV) or other additional technologies.

1.3.3 Metabolite separation and analysis

Several chromatographic and electrophoretic methods such as LC and CE, with various detection techniques such as UV and MS, have been used for the identification and structural validation of nucleotide sugars and nucleotides[71,72]. CE-UV allows effective separation with reliable detection of known compounds within a sample. By adding a standard into a mixture that contains the compound represented by the standard, the identity of a constituent of a peak can be confirmed. Further, the development of standard curves allows specific compounds to be quantified[73].

Feng *et al.* were the first to report highly effective separation for the simultaneous quantification of intracellular nucleotide and sugar nucleotide analysis (Figure 7[72]). As CE is a highly sensitive technique, a variety of CE operating conditions must be optimised including buffer pH value, voltage, capillary temperature, capillary coating and the sample extraction protocol. The CE separation method described in [73] resulted in successful identification and quantification of all 12 common nucleotides and seven sugar nucleotides from CHO cells. This method was therefore chosen for the analysis of key nucleotides and nucleotide sugars in *T. reesei* after growth in the two chosen media, which differed only in carbon source.

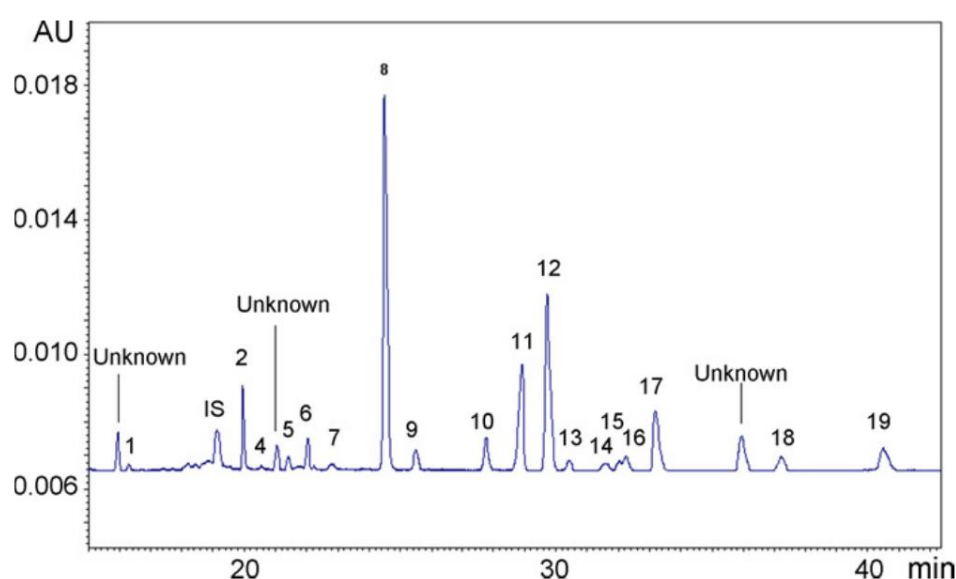


Figure 7 - CE-UV electropherogram from CHO cell extract. Buffer: 40mM borate buffer (pH 9.50) with 1.0% (w/v) PEG addition. Total length of capillary: 75cm. Separation temperature: 22 °C. Peaks from left to right in electropherogram (A): 1, CMP-NeuAc; 2, UDP-GlcNAc; 3, GDP-Man; 4, GDP-Fuc; 5, UDP-Glc; 6, UDP-GalNAc; 7, UDP-Gal; 8, AMP; 9, CMP; 10, GMP; 11, ATP; 12, ADP; 13, GTP; 14,CTP; 15, CDP; 16, GDP; 17, UMP; 18, UTP; 19, UDP[72].

1.4 Evaluation of protein N- and O-glycosylation

A variety of chemical and enzymatic methods are used to release *N*- and *O*- glycans from proteins for glycoproteomics[74]. The removal of *N*-linked glycans from proteins is facilitated by the use of the endoglycosidase peptide-*N*-glycosidase F (PNGase F). This enzyme cleaves the bond between the asparagine residue of the glycosylated protein and the reducing GlcNAc of the attached *N*-linked glycan[75]. Following *N*-glycan release, reductive β -elimination can

then be used to release *O*-glycans from the same proteins[74]. This chemical method involves an alkaline reaction which cleaves the *O*-glycan-peptide bond. The reducing terminus is then reduced to prevent alkaline degradation[75]. Following the release of the attached *N*- and *O*-glycans, these oligosaccharides are typically analysed by mass spectrometry.

Separation and analysis of released *N*-linked and *O*-linked glycans can be conducted using porous graphitised carbon (PGC) - electrospray ionisation (ESI) - tandem mass spectrometry (MS/MS)[76–79]. Compared to other chromatographic techniques, PGC has been found to effectively and reliably separate non-derivatised oligosaccharides, especially enabling the high resolution of structural isomers[80]. This high resolution combined with reliability of elution order allows the establishment of mass-composition-retention time correlations[81], and when coupled to ion-trap tandem mass spectrometry, structural information can be determined from the diagnostic fragmentation ions[55,78]. This robust technique provided an effective tool for the analysis of the glycosylation of secreted proteins of *T. reesei* for this thesis, allowing investigation of the effect of carbon source on protein glycosylation, and correlation with the associated metabolites involved in glycan biosynthesis.

1.5 Research aims

The overall aim of this research was to examine the effect of carbon source on the protein glycosylation pathway of *Trichoderma reesei* RUT-C30. To achieve this, the specific goals were to:

- (i) determine of the effect of glucose and lactose as sole carbon sources on the physiological status (pH, mycelial growth, protein secretion and CBHI activity) of *T. reesei*;
- (ii) develop an extraction procedure for nucleotides and nucleotide sugars in *T. reesei*
- (iii) profile the nucleotide sugar and nucleotide levels in *T. reesei* when grown in liquid media containing either glucose or lactose as sole carbon source; and
- (iv) profile the *N*-glycans and *O*-glycans attached to secreted glycoproteins produced by *T. reesei* when grown in liquid media containing either glucose or lactose as sole carbon source.

Chapter 2 - Materials and Methods

2.1 Chemicals, proteins and other materials

All chemicals were sourced from Sigma Aldrich (Sydney, Australia) unless otherwise specified. Biolog FF MicroPlates were from Biolog Inc. (Hayward, USA), peptide-*N*-glycosidase F (PNGase-F) was from Roche Applied Science (Sydney, Australia), Trypsin was from Promega Corp. (Sydney, Australia) and all Milli-Q water was obtained using a Millipore Academic Milli-Q system. For polar metabolite analysis, target components included 3 nucleotides [adenosine 5- monophosphate (AMP), adenosine 5-diphosphate (ADP) and adenosine 5-triphosphate (ATP)] and 7 nucleotide sugars [UDP-glucose (UDP-Glc), UDP-*N*-acetyl-glucosamine (UDP-GlcNAc), GDP-fucose (GDP- Fuc) and GDP-mannose (GDP-Man)] purchased from Sigma Aldrich (Sydney, Australia). All nucleotides and sugar–nucleotides standards were prepared in Milli-Q water and stored at –30°C. Sodium tetraborate and sodium hydroxide used for capillary electrophoresis were from Agilent Technologies (CA, USA).

2.2 Fungal strain

The fungal strain studied was *T. reesei* RUT-C30 (ATCC 56765)[82], and was maintained on Potato Dextrose Agar (PDA) plates.

2.3 Biolog assay

Carbon source utilisation was evaluated by using Biolog FF MicroPlate (Biolog Inc., USA). The FF MicroPlate test panel contains 95 wells, each with a different carbon source, and one well with water. *T. reesei* RUT-C30 was grown on PDA plates in the dark at 28 °C for five days. The culture plates were then placed by the windowsill in the lab for two days to induce sporulation through sunlight exposure. Conidia were collected using a cotton swab moistened with collection medium (0.25% Phytigel, 0.03% Tween 40). The conidia were suspended in the collection medium and adjusted to an absorbance at 600 nm of 0.75 ± 0.01 . Following this, 90 µL of the conidial suspension was dispensed into each well of the FF Microplate.

The FF plates were incubated in the Omnilog automated plate reader for 48 hours at 30 °C and the change in dye colour, due to reduction of tetrazolium dye resulting from carbon

source breakdown, was recorded every 15 minutes which resulted in the generation of a carbon utilisation curve. RUT-C30 was analysed with two independent experiments using separately prepared inoculum. Data analysis was performed using Kinetic and Parametric software (Biolog Inc., USA).

2.4 Liquid cultivation in shake flasks

Prior to liquid cultivation in shake flasks, RUT-C30 was cultivated on PDA for 5 days, as described above. Conidia were collected by adding a 0.9 % NaCl / 0.01 % Tween 80 solution and then gently scraping the surface of the PDA plates with a bent glass rod. The conidial suspension was filtered through 5 mL pipette tips packed with glass wool to remove hyphae, and the concentration of conidia in the filtrate was calculated using a haemocytometer. Conidial suspensions were stored either at 4 °C temporarily or at -80 °C in 12.0 % (v/v) glycerol/0.04 % (v/v) Tween 80 solution for extended periods.

Cultivation was conducted in 250 mL shake flasks containing 50 mL of minimal medium with either lactose or glucose as a carbon source. Preparation of the minimal salt medium is described in Penttilä *et al.*[27]. The medium contained (per litre) 15 g KH_2PO_4 , 5 g $(\text{NH}_4)_2\text{SO}_4$, 10 mL 100 x trace elements (100 mg $\text{FeSO}_4 \times 7\text{H}_2\text{O}$, 20 mg $\text{MnSO}_4 \times \text{H}_2\text{O}$, 20 mg $\text{ZnSO}_4 \times 7\text{H}_2\text{O}$, 40 mg $\text{CoSO}_4 \times 7\text{H}_2\text{O}$ in 200 mL Milli-Q water) with the pH adjusted to 6.5 with 10 M KOH. The solution was autoclaved at 121°C for 20 min before adding (per litre) 50 mL 20 % (w/v) lactose or glucose (depending on carbon source), 2.4 mL 1 M MgSO_4 and 5.4 mL 1 M CaCl_2 , which were sterilised separately. After cooling, 50 mL of the medium was allocated to each flask and inoculated with 1×10^8 of freshly harvested conidia which were counted using a haemocytometer. Cultures were incubated for seven days at 28 °C in the dark with constant agitation at 250 rpm. Samples (3mL) were taken from each flask, each day, over four days for analysis of culture pH, secreted protein and mycelial growth.

2.5 Monitoring of culture pH and mycelial growth

The pH was measured from daily culture samples using a thin pH probe (Mettler Toledo, Australia) with calibration before analysis. The fungal growth rate was determined by measuring the mycelial dry weight as described by Kubicek[83]. For each biological replicate, 1 mL of each culture sample was placed on pre-weighed and pre-wet 5.5 cm ash-less filter paper (Whatman Ltd, Australia). The filter containing the mycelia was washed three times

with Milli-Q water and left to dry for 48 hours at 70 °C. The dry weight of the mycelia was determined by subtracting the original weight of the filter paper (above) from the weight of the filter paper with dried mycelia.

2.6 CBHI activity

To separate the culture supernatant from the cell mass, the daily culture samples (1 mL) were centrifuged at 13,000 rpm for 5 min. The supernatant was collected and then stored at -80 °C. The assay for CBHI activity was performed with adaption to the 96-well plate protocol by Xue (2012). Briefly, 10 µL of culture supernatant was added to 100 µL of 1 mM 4-methylumbelliferyl β-D-cellobioside in 50 mM sodium-citrate buffer, pH 6.0, and 1 mM dithiothreitol (DTT). The reaction was incubated at 40 °C for 1 hour with gentle agitation and terminated by adding 25 µL of 1M Na₂CO₃. The assay was performed with technical and biological triplicates and fluorescence of the cleaved substrate was measured using a Fluostar microplate reader (BMG, Australia) at excitation and emission wavelengths of 365 nm and 455 nm respectively. Milli-Q water was used in place of the 10 µL culture supernatant in the above procedure to provide a background reading without CBHI activity.

2.7 Protein concentration

The Bradford assay was used to quantitate the concentration of secreted protein in the culture supernatants using Bradford reagent (Sigma, Australia)[84]. Bovine serum albumin (BSA) (Sigma, Australia) was prepared with a series of dilutions from 0 to 1.25 mg/ml and these dilutions were used as a standard for the assay which was conducted according to the manufacturer's instructions. To concentrate the samples for quantification by the Bradford assay, secreted proteins were precipitated from the culture supernatant using a 9:1 ratio of ice cold acetone to supernatant and left overnight at -20 °C. The protein was centrifuged at 13,000 rpm for 5 min to form a pellet and acetone was removed, with washing with acetone and centrifuging performed twice to reduce the influence of the variable cellular metabolites. The pellet was left to dry, and then was resuspended in 4 M urea (Sigma, Australia) to a recorded volume less than the original culture supernatant sample (representing the concentration factor), prior to analysis with the Bradford assay. The assay was performed with technical and biological triplicates and measured in a spectrophotometer with absorbance at 595 nm. The protein concentrations of the culture supernatants were then calculated based on the concentration factor.

2.8 Extraction of nucleotides and nucleotide sugars

2.8.1 Quenching fungal cells and extraction of polar metabolites

Trichoderma reesei RUT-C30 was grown as previously described (Section 2.4). Quenching of cells and extraction of intracellular metabolites was adapted from de Koning and Van Dam[85]. Fungal mycelia were collected in 1 mL aliquots and added to 1.5 mL of ice-cold 60% methanol to quench and wash the cells. The cells were pelleted by centrifuging for 5 min at 5,000 rpm and 4 °C. The supernatant was discarded and the pellet was resuspended in 2 mL of ice-cold extraction solution composed of 1 mL chloroform, 0.5 mL methanol and 0.5 mL of aqueous buffer (3 mM piperazine-N,N'-bis (PIPES), 3 mM ethylene-diamine-tetraacetic acid (EDTA) and pH 7.2).

The cells were shaken at 125 rpm for 45 min at 4°C in the extraction solution with initial vigorous manual shaking. The separation of the polar (upper phase), non-polar (lower phase) and cell debris was achieved after centrifugation at 5,000 rpm for 5 min at 4 °C. The polar metabolites, found in the upper aqueous phase, were collected whilst ensuring the remaining fractions were not disturbed. Any fine particulate matter was removed by passing the collected polar fraction through a 20 µm filter and then frozen at -80 °C. If samples required concentration, they were concentrated using a vacuum concentrator (Christ, Germany) followed by centrifugation at 13,000 rpm for 10 min at 4 °C to pellet any fine precipitates from the concentrated cell extract.

2.8.2 Capillary electrophoresis with diode array detection

The CE separation was performed on an Agilent 7100A capillary electrophoresis instrument (Agilent Technologies, USA). A 50 µm diameter capillary with an effective length of 56 cm was used for separation using 50 mM sodium tetraborate, pH 9.3. The analysis was performed based on the protocol by Feng *et al.* with modifications[72]. Before daily runs, the capillary was rinsed for 10 min with 1 M NaOH, 10 min with water, and 10 min with running buffer. Running buffer was replenished after every run for reproducible migration times. To condition the capillary before each run, the capillary was washed for 5 min with buffer and following each run, the capillary was washed with 1 M NaOH for 5 min, followed by running buffer for 5 min. Samples were introduced from inlet side at 30 mbar for 15 sec. The separations were performed under a constant voltage of 22 kV for 40 min and detection of metabolites visualized at 260 nm with 10 nm bandwidth.

Peak area and migration time determination was performed using ChemStation (Agilent Technologies, USA) using the AutoIntegrate function with manual annotation when required. The data was manually calculated into relative abundances of each nucleotide sugar based on peak area. Biological replicates were analysed according to average migration times and relative abundances of each nucleotide sugar.

2.8.3 Analysis of the ATP standard using mass spectrometry

Analysis of the ATP standard (Sigma, Australia) was performed by mass spectrometry to determine purity. The standard was prepared to a concentration of 1 nmol/L in 50 % Milli-Q water and 50 % acetonitrile (v/v) and directly injected into the ESI source of an Ion-Trap mass spectrometer (Agilent 6330, Agilent Technologies, USA). In the ion-trap mass spectrometer, the capillary was maintained at 300 °C and the outlet was set to a voltage of 3 kV. The mass spectra were obtained in negative ion mode using a mass range of between m/z 200 and 2200. Ions were detected in ion charge control (ICC) with a target of 80,000 ions and an accumulation time of 200 milliseconds. Induced collision was performed at 35 % normalised collision energy and an isolation window of 4 m/z . Single ion monitoring of the following negative ions ± 0.3 Da: 346.0 Da, 426.0 Da and 505.0 Da was performed. These masses were chosen as they correspond to the appropriate m/z values for AMP, ADP and ATP. Relative abundances of the ions were determined by the relative intensities at 2.75 min, the time at which the injected sample was analysed by the Ion-Trap.

2.9 Sodium dodecyl sulphate polyacrylamide gel electrophoresis (SDS-PAGE) and protein identification by mass spectrometry

Casting and electrophoresis of 10% Bisacrylamide-Tris SDS gels was performed according to the method of Royle *et al.*[75]. All materials used to make the gel were from Sigma Aldrich (Sydney, Australia). The protein electrophoresis was conducted to analyse the secreted protein profile from the culture media, with a focus on CBHI which has an expected mass of 57 kDa without any post-translational modifications[19]. This major band on the gel was also used to verify the identification of CBHI by mass spectrometry and as a source of *N*-linked glycans attached to the major secreted *T. reesei* cellulase.

The samples, composed of 30 μ g of secreted protein, were prepared by acetone precipitation as described previously (Section 2.7), reduced and alkylated then loaded into

each lane with a Tris-Glycine loading buffer based on the protocol by Laemmli[86]. In addition, 10 µg of bovine fetuin (Sigma, Australia), a glycoprotein standard, was added as a control for the *N*-glycan release. The gel bands were cut out and prepared according to Royle *et al.*[87], with *N*-glycans released using PNGase-F (Roche, Australia) at 37 °C overnight and extracted using acetonitrile. The purified *N*-glycans were then stored at -30 °C until later analysis (Section 2.10.2). The *N*-deglycosylated protein contained in gel bands was then digested with Trypsin at 37 °C overnight (Promega, Australia) and resulting peptides were extracted from the gel using acetonitrile and dried with SpeedVac. The dried peptides were then reconstituted in 10 µL Milli-Q water and placed in liquid chromatography – mass spectrometry vials (Water, Australia) for protein identification by mass spectrometry.

The released peptides were analysed with liquid chromatography – electrospray ionisation – tandem mass spectrometry (LC-ESI-MS/MS) run on a Q-Exactive mass spectrometer (Thermo Scientific, Australia). Samples were injected into a room temperature column using a 0.1% formic acid solvent. The separation was performed using high performance liquid chromatography (HPLC) with a reversed phase C-18 column using 0.1 % formic acid (Buffer A) and 99.9% acetonitrile with 0.1% formic acid (Buffer B) with a flow rate of 300 nL/min. The gradient was 1% Buffer B to 50% Buffer B across 30 min, then to 85% Buffer B for 2 min, then held at 85% Buffer B for a total run time of 40 min.

The column eluent was directly ionised at 1.6kV with a capillary temperature of 250 °C. The C-trap accumulation time for the detection of ions was 120 ms maximum for MS and 60 ms maximum for MS/MS. For MS/MS, HCD-energy was set to 30 eV with an isolation window of 3.0 m/z. Database searching and result filtering were performed with Proteome Discoverer (Thermo Scientific, Australia) against the SwissProt fungal database using Mascot. Search parameters can be found in the Supplementary section 7.5.

2.10 N-glycan and O-glycan analysis of secreted proteins

2.10.1 Protein immobilisation and N-glycan/O-glycan release

N- and *O*-linked glycans were released from secreted proteins according to Jensen *et al.*[75]. Based on the previously determined secreted protein concentrations for each cell culture supernatant, 5 µg of total secreted protein was precipitated and washed with acetone as previously described. The equivalent aliquots of protein, from each biological replicate, were

immobilised onto Immobilon-P polyvinylidene fluoride (PVDF) membranes (Millipore, Australia) using dot blotting to prepare for glycan release. PNGase F (3 units) was added to each dot blot and incubated overnight at 37 °C to release the *N*-linked glycans. To remove glycosylamines from the reducing terminus of released *N*-linked glycans, 100 mM ammonium acetate pH 5 (final concentration 15 mM) was added and incubated for 60 min at room temperature, and dried in a vacuum centrifuge. To reduce the released *N*-glycans, 1 M NaBH₄ in 50 mM KOH was added and incubated at 50 °C for 3 hours. Glacial acetic acid was added to neutralise the reaction and purification of *N*-linked glycans was performed using AG50W-X8 cation-exchange resin (BioRad, USA) packed in C18 ZipTips (Thermo Scientific, Australia) to desalt the prepared *N*-glycans. To remove the residual borate from the glycan samples, methanol was added and dried under vacuum thrice.

To release *O*-linked glycans, reductive β -elimination was performed on the PNGase F treated proteins with incubation of the PVDF spots overnight in 0.5 M NaBH₄ in 50 mM KOH at 50 °C for 16 hours. The reduction was neutralised with glacial acetic acid and *O*-linked glycans were purified using cation exchange columns as previously described for the *N*-glycans. The purified glycans were reconstituted in Milli-Q water and analysed by porous graphitized carbon (PGC) LC-ESI-MS/MS.

2.10.2 Mass spectrometric analysis of released glycans

The released *N*-glycans and *O*-glycans were separated using a 5 μ m Hypercarb PGC column (Thermo Hypersil, Runcorn, UK) maintained at 27 °C. The samples were injected onto the PGC column in 10 mM ammonium bicarbonate, pH 8. Separation of *N*-glycans was performed over an 85 min gradient of 0–45% (v/v) acetonitrile in 10 mM ammonium bicarbonate. Similarly, the elution of *O*-glycans was performed over a 45 min gradient of 0–90% (v/v) acetonitrile in 10 mM ammonium bicarbonate. Using a HPLC system (Agilent 1100, Agilent Technologies, USA), a flow rate of 2 μ L/min was used to separate both the *N*- and *O*-glycans and the eluent was introduced directly into the ESI source (Agilent 6330, Agilent Technologies, USA).

In the ion-trap mass spectrometer, the capillary was maintained at 300 °C and the outlet was set to a voltage of 3 kV. The mass spectra were obtained in negative ion mode using a mass range of between *m/z* 200 and 2200. Ions were detected in ion charge control (ICC) with a

target of 80,000 ions and an accumulation time of 200 ms. Induced collision was performed at 35% normalised collision energy and an isolation window of 4 m/z.

2.10.3 Data Analysis

The resulting glycan tandem mass spectra were manually annotated based on published *N*-glycan and *O*-glycan compositions/structures as well as available biological pathways on KEGG[21,54,55,78]. Structural feature ions, allowing identification of the number of antennae, was based on Harvey's work with high mannose *N*-linked glycans[55]. The annotation and interpretation of fragment ion spectra, to determine composition and sometimes structure, was further characterized with the assistance of software tools, GlycoMod[88] and GlycoWorkBench[89]. All glycan compositions (Hexose, HexNAc, HexA) were confirmed with MS² and masses with retention times of ± 0.2 min had to be found in at least 2 biological replicates for each culture condition.

Chapter 3 Results

To monitor the effect of carbon source on the physiology and glycosylation pathway of *Trichoderma reesei* RUT-C30, data was collected in three areas: (i) physiological analysis, including carbon source utilisation (Biolog assay); and mycelial growth, pH of culture media, protein secretion and CBHI activity (shake flasks); (ii) glycomic analysis of the secreted proteins; and (iii) metabolite analysis, namely nucleotide and nucleotide sugar abundance in the fungal mycelia. These areas of interest were monitored because each one may contribute to, or represent, the protein glycosylation pathway to some degree.

3.1 Physiological studies

3.1.1 Biolog assay for carbon utilisation

To assess the utilisation of various carbon sources by RUT-C30, the strain was screened using two Biolog filamentous fungi (FF) microplates (Supplementary figures I, II and III). These plates are often used for microbe identification based on the carbon utilisation curves but also have been used to understand more about the capabilities of the organism of interest[66]. In the analysis presented here, particular attention was paid to the utilisation of carbohydrates that could be used in a culture medium to support fungal growth, and sugars that are known constituents of *N*- and *O*-linked fungal glycans[90–92] .

Two biological replicates of RUT-C30 were screened for carbon utilisation with Biolog FF microplates for 48 hours, with this length of incubation based on previous Biolog work with other *T. reesei* strains[66]. The area under the carbon-breakdown curves (indicated by reduction of the tetrazolium) was used to compare utilisation of seven carbon sources of interest, and normalised against redox reactions (theoretically zero) in a well containing only water (Figure 8). There was no significant difference between the reduction of tetrazolium in wells containing water and those containing lactose or galactose, implying that the inoculated fungi did not breakdown these carbon sources for energy production within the 48 hour period. However, significant breakdown of cellobiose, glucose and mannose was observed, and utilisation of *N*-acetyl glucosamine (GlcNAc) was suggested, although variations in the data between the two biological assays caused a loss of statistical validity (Figure 8).

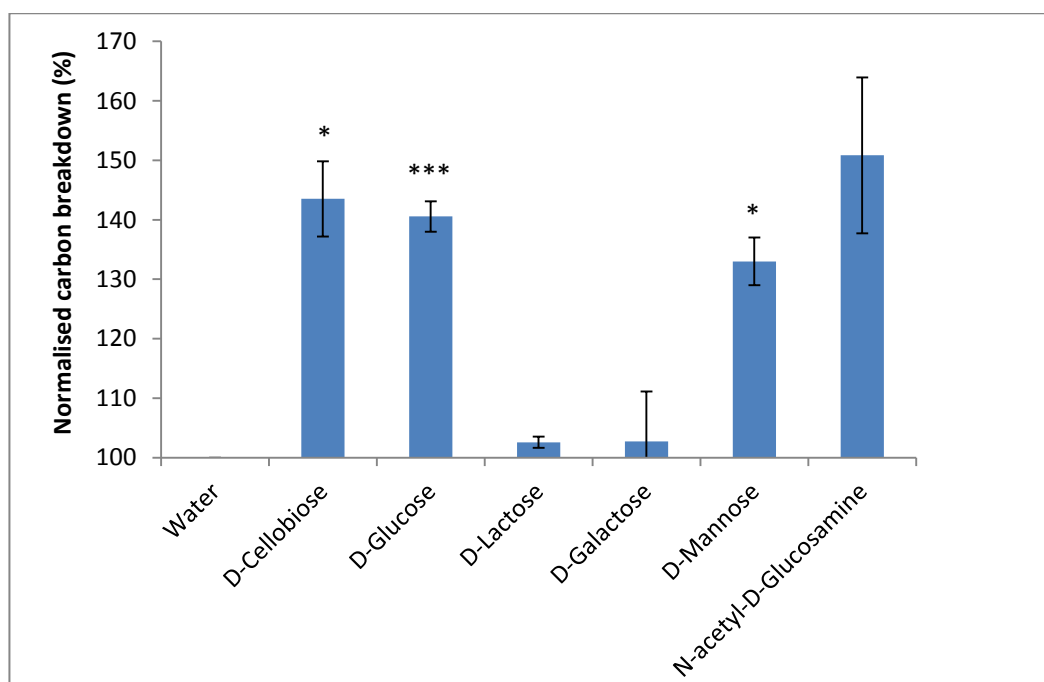


Figure 8 - Carbon utilisation of *T. reesei* RUT-C30 over the first 48 hours of growth on selected carbohydrates in the Biolog assay. Carbon utilisation, indicated by reduction of tetrazolium, was calculated by area under the curve using two biological replicates and compared to tetrazolium reduction when grown on water only, normalised as 100. Significant differences in utilisation of carbon source, compared to water, is indicated by (*) $p < 0.05$, () $p < 0.01$ and (***) $p < 0.005$.**

The Biolog assay provided insight into carbon utilisation by RUT-C30 in the first 48 hours after conidial inoculation, and it was particularly intriguing that utilisation of lactose was not indicated during this time, despite knowledge of lactose as an inducer of CBHI production[91] (discussed further in section 4.1). In the next phase of experimental work, cultivation of RUT-C30 was carried out using glucose and lactose as sole carbon sources in larger scale shake flask cultures over five days, enabling regular monitoring of mycelial growth and the pH, secreted protein concentration and CBHI activity of the culture supernatant, as well as glycomic analysis of the secreted proteins.

3.1.2 Mycelial growth and pH of shake flask cultures with glucose or lactose as sole carbon source

There are several factors that can influence cellulase production and growth by *T. reesei* RUT-C30 including carbon source, temperature and pH [93]. Whilst some of these factors, such as temperature and carbon source can be controlled in shake flask growth, other factors need to be monitored externally, including pH. Culturing of *Trichoderma reesei* RUT-C30 was performed as described in the methods, with six flasks in total: three shake flasks

contained minimal medium with glucose as a sole carbon source, and three shake flasks contained minimal medium with lactose as a sole carbon source. A total of 3 mL aliquots were taken from each culture flasks each day, for four days. The first 1 mL was used for determining mycelial growth rate. The second 1 mL was used for pH and secreted protein and glycan analysis. The third 1 mL was used for metabolite analysis.

The growth rate of the filamentous fungi cannot be accurately determined using optical density at 600 nm measurements, which is usually performed for bacterial cultures, due to non-uniform distribution of filamentous fungi in culture[94]. As an alternative, mycelial dry weight was used to determine the cell density in the culture medium. The pH was also monitored because it is an indicator of growth and metabolic activity, and is also known to have an impact on the production and catalytic activity of secreted enzymes of RUT-C30, including secreted proteases and glycosidases[23,93].

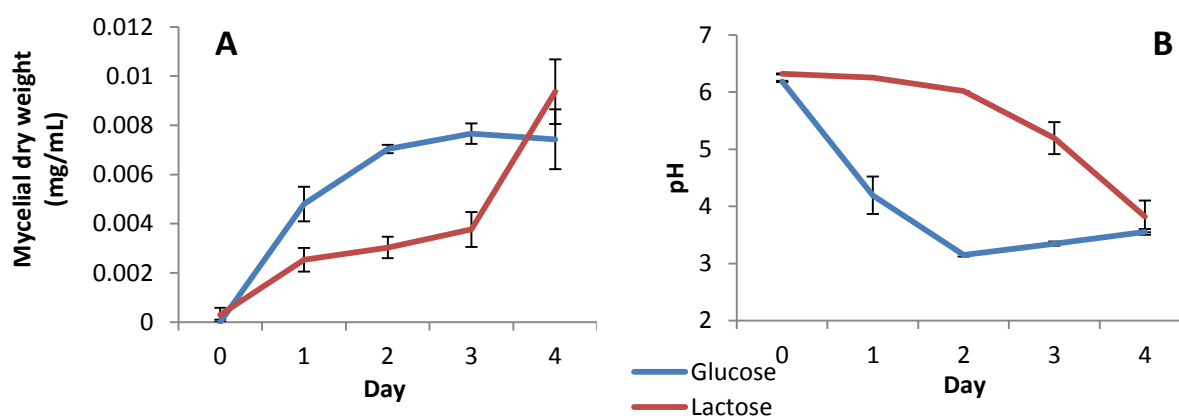


Figure 9. Indicators of growth for *T. reesei* RUT-C30 cultures with glucose and lactose as sole carbon source: (A) Mycelial dry weight from culture, (B) pH of culture supernatant.

As seen in figure 9 (A), the glucose and lactose cultures featured very different growth patterns. Starting from day 0, the mycelia in the glucose culture grew rapidly then growth seemed to plateau from day 2 onwards. The lactose culture took three days before mycelial growth increased exponentially which correlates with the 48 hour Biolog assay data. The pH fluctuation (Figure 9 B) appeared to mirror the mycelial growth, with acidification of the lactose culture medium occurring at a slower but constant rate while the glucose culture featured a faster acidification with a plateau at pH 3.0 – 3.5 from day 2. By the fourth day, there was no significant difference in mycelial dry weight or pH despite the differences over the first, second and third days of culturing.

3.1.3 Protein secretion and CBHI activity in the culture supernatants

Supernatants from the flask cultures with glucose and lactose as sole carbon source (section 3.1.2) were regularly assessed for total protein concentration and CBHI activity. As well as monitoring the protein secretion rate, assessment of the protein concentration of the supernatant was essential for the experimental workflow as it allowed known amounts of protein to be used for *N*- and *O*-glycan analysis (section 3.3).

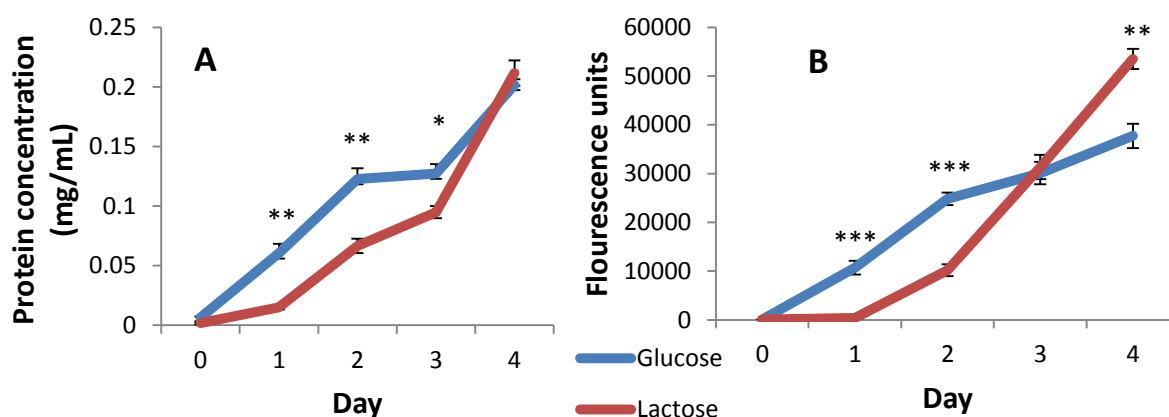


Figure 10. Protein concentration (A) and CBHI activity (B) of the supernatants of RUT-C30 grown on glucose and lactose as sole carbon source: Protein concentration calculated with Bradford assay. Relative CBHI activity determined by breakdown of fluorescently labelled cellobiose. Significant differences in the protein concentration or CBHI activity according to carbon source are indicated (*) $p < 0.05$, () $p < 0.01$ and (***) $p < 0.005$.**

From day one through to day three, overall protein secretion was significantly higher in the glucose cultures than in the lactose cultures, with no significant difference on the fourth day (Figure 10 A). There also appeared to be a slowing rate of protein secretion between day 2 and 3 for both cultures. CBHI activity (Figure 10 B), was also significantly higher in the glucose cultures on days 1 and 2; however, the CBHI activity rapidly increased in the lactose culture after day 2, became equal to the glucose culture on day 3, and significantly higher than in the glucose culture on day 4.

Precipitated protein from day four culture supernatants grown on both carbon sources was run on SDS-PAGE gels to confirm CBHI was the most abundant protein in the culture supernatants. The darkest gel band appeared at the expected molecular weight of CBHI, was excised from each lane and digested by trypsin for protein identification by LC-ESI-MS/MS as

described in the methods. Following data analysis, the band was identified to be mainly CBHI in addition to the presence of other carbohydrate degrading enzymes; thereby confirming that CBHI was the most abundant protein expressed on day four of cultivation in both glucose and lactose cultures. The gel image and protein identification results can be found in the Supplementary section (Section 7.5).

3.2 Analysis of nucleotides and nucleotide sugars

In order to measure the energy status and nucleotide sugar pools of RUT C30 grown on glucose or lactose, the 1mL sample taken from culture flasks each day was washed, quenched, extracted and analysed using CE-UV as described in the methods section (Section 2).

Three nucleotide sugars that are the precursors of the identified fungal glycans (UDP-GlcNAc, GDP-Man, UDP-Glc) and two energy based nucleotides (AMP, ADP) were able to be identified in the samples, based on spiked standards (Figure 11 and Supplementary figure V). The electropherograms demonstrated effective separation of elution peaks, and identification of all intracellular metabolites of interest (except for ATP) was achieved.

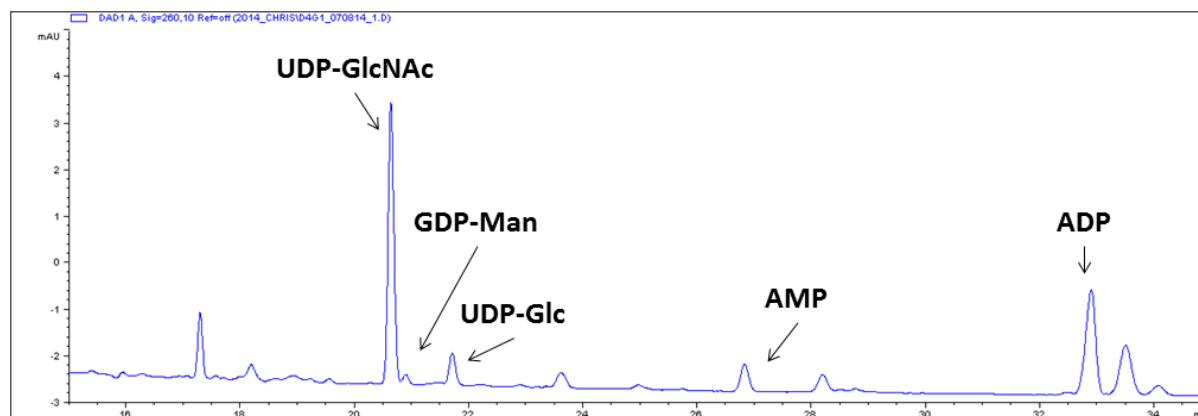


Figure 11. Example electropherogram of extracted polar metabolites from *T. reesei* RUT-C30. Extraction was performed using chloroform:methanol:water extraction. Peak identities were determined using spiking of standards, demonstrated in the Supplementary Figure V.

3.2.1 CE-UV method development for metabolite analysis.

A limit of detection of 1 μ M of each nucleotide sugar was determined for this method, and the concentration of GDP-Man in the prepared samples was below this threshold, therefore unable to be detected in the culture samples on all days except for day 4 (data not shown).

As a result, concentration of samples was performed when required. To identify the optimal method to use, Speedvac vacuum concentration and freeze drying were compared for their capacity to concentrate mixtures of nucleotide sugar standards UDP-GlcNAc, GDP-Man and UDP-Glc. The mixtures were concentrated until dryness, reconstituted in Milli-Q water and then subjected to CE-UV. Figure 12 shows the peak areas corresponding to each standard nucleotide sugar following concentration by each method, demonstrating that the Speedvac was more effective for concentration of the sample while reducing sample loss. For this reason, SpeedVac was chosen as the method to use to concentrate samples for optimal measurement of low abundance nucleotide sugars.

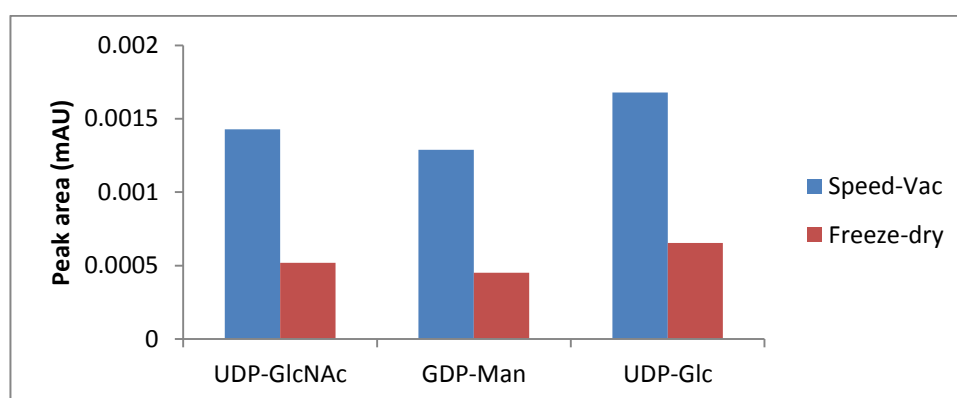


Figure 12. Comparison of concentration techniques for sample preparation of a standard mixture containing nucleotide sugars of interest.

As previously mentioned, ATP was not able to be identified in the RUT-C30 extracts using CE-UV and standard spiking. When an ATP standard was added to an extract with all other metabolite peaks identified, ADP and AMP peaks increased in area. This was unexpected as this method had resulted in effective separation of ATP, ADP and AMP in previous literature[72]. Two possibilities existed to explain this result: i) co-elution of ATP with ADP or (ii) the ATP standard had been degraded to ADP and/or AMP. To identify if the problem had been due to co-elution, a sample was run at half the voltage with double the run time to improve resolution but had no effect on resolving additional peaks.

To assess the quality of the ATP standard, Multiple Reaction Monitoring (MRM)-MS using an ion-trap was performed as described in the methods, with a focus on the possible identification of AMP, ADP and ATP. From this analysis it became evident that the largest component of the commercially freshly supplied “ATP” standard was actually ADP, making up 65% of the standard, followed by AMP (25%) and then ATP (10%) as shown in figure 13.

Combining this result with the previous CE-UV analysis of the standard, it was then evident that the ATP had degraded to form ADP and AMP.

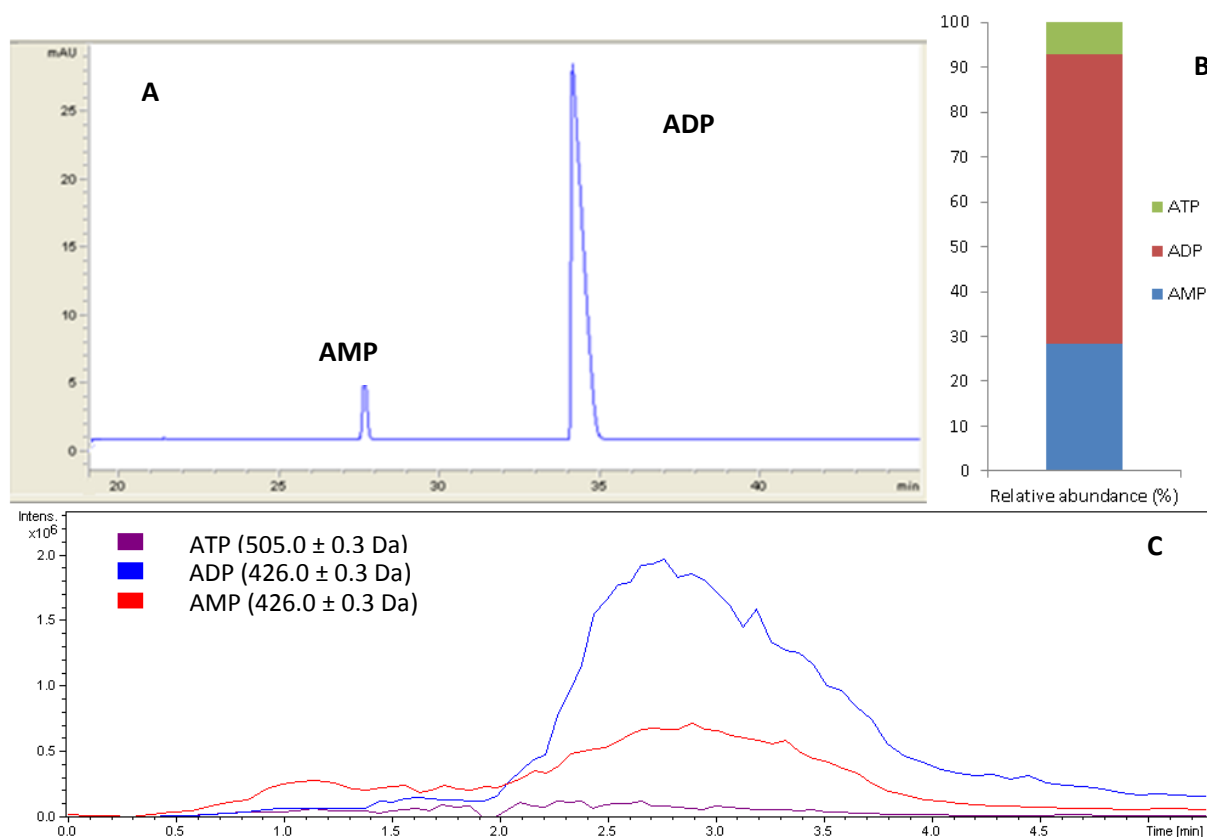


Figure 13. (A) CE-UV electropherogram of ATP standard (Sigma, 98% purity) that was to be used to identify ATP peaks in the RUT-C30 extracts, (B) Relative abundances of ATP, ADP and AMP in the ATP standard determined by MRM MS based on peak area, and (C) selected ion monitoring of ATP, ADP and AMP in the MS analysis.

3.2.2 Comparison of nucleotide-sugar and nucleotide pools in RUT-C30 grown on glucose and lactose

From the analysis of the nucleotide sugars in the cells, shown in figure 14, there was no significant difference in relative abundance of UDP-GlcNAc between growth on carbon sources on day 1, but every day after that the cell extracts from the glucose cultures had a significantly higher UDP-GlcNAc content than the cell extracts from the lactose cultures, with the greatest difference occurring on day 4 (Figure 14A). This is contrasted by the abundance of GDP-Man, which was significantly higher in the glucose cultures on day 1, but significantly lower on day 4 than in the cells grown with lactose, with no significant difference on the other days (Figure 14B). Figure 14C shows there was a significantly higher abundance of UDP-Glc in the cell extracts from the lactose cultures from day 2 onwards when compared to

that in the glucose grown cultures. For each nucleotide sugar, the greatest difference in relative abundance was found on day 4.

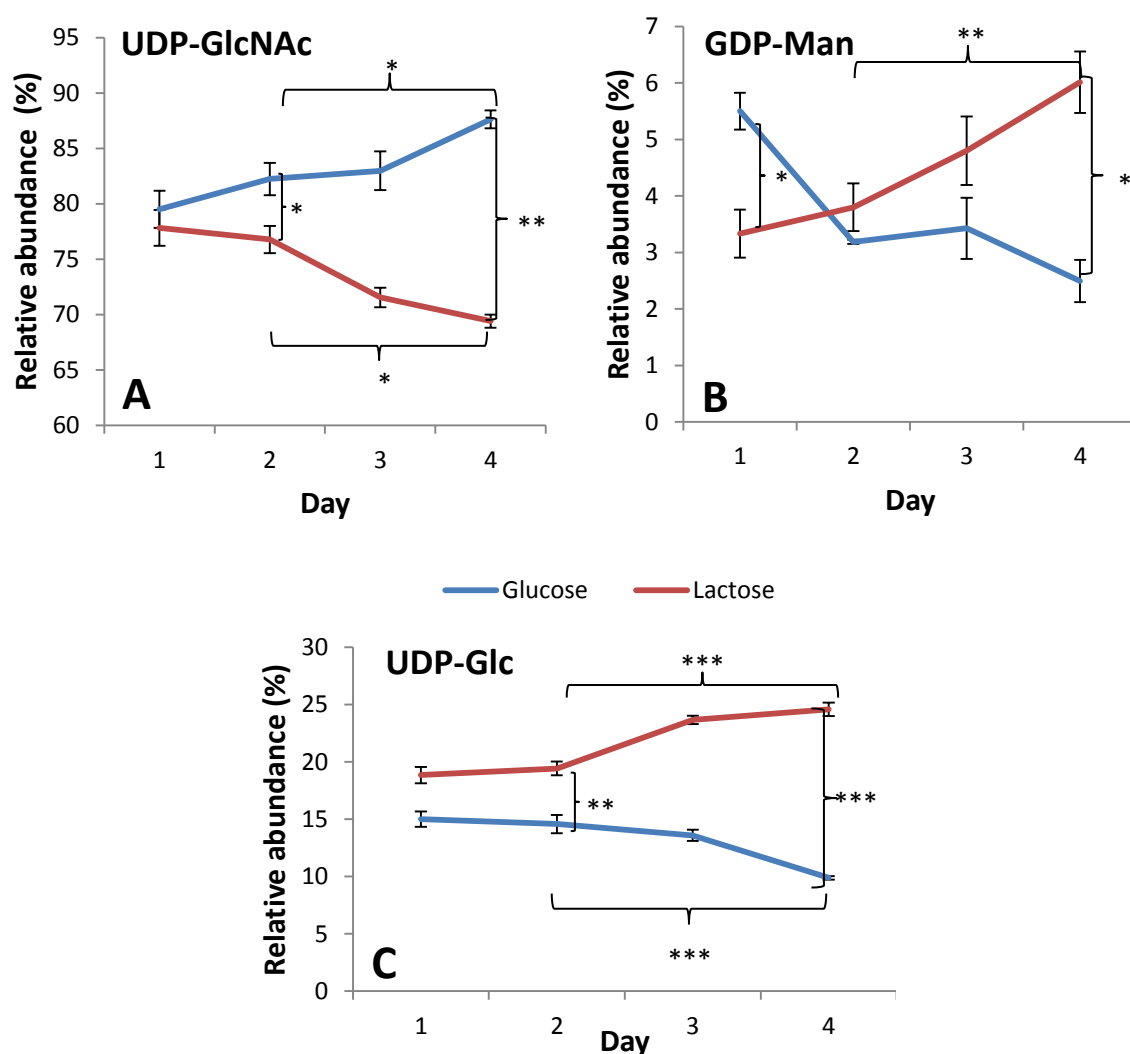


Figure 14. Relative abundances of intracellular nucleotide sugars in *T. reesei* RUT-C30 over four days using glucose or lactose as sole carbon sources. (A) UDP-GlcNAc (B) GDP-Man (C) UDP-Glc. Significant differences in relative abundance between the two carbon sources are indicated (*) $p < 0.05$, (**) $p < 0.01$ and (***) $p < 0.005$.

3.3 *N*-glycan and *O*-glycan analysis of secreted proteins

As the glycosylation of the total protein complement secreted from the cell represents the products of the complete glycosylation pathway, including the energy state and nucleotide sugar precursor pools, the *N*- and *O*- glycan structures were analysed as a measure of the protein glycosylation status by growth on the two carbon sources.

Challenges for glycan analysis in mass spectrometry include the identification of isomers which are glycans with the same mass and composition that vary in sequence of branching structure. For monosaccharide compositional determination from mass, the hexoses glucose, galactose and mannose have the same mass, sometimes requiring the use of monosaccharide analysis to confirm their identity. Similar difficulties are faced for phosphorylation and sulfation with both having approximately the same mass, requiring separation by charge to effectively determine identity. In the case of the oligosaccharide glycans, tandem MS (MS/MS), together with knowledge of established glycosylation pathways and the use of glycan databases with previously identified structures, need to be used for manual assignment of putative glycan structures.

Glycomic analysis by MS revealed there was no significant difference in the *N*-glycan structures from the major band identified as CBHI separated by SDS-PAGE gel and from total secreted proteins, using day 4 cultures (data not shown). As CBHI is a glycoprotein and has been documented to make up 50-60% of secreted protein of *T. reesei*, the total secreted protein glycosylation was used for *N*-glycan and *O*-glycan analysis.

Day two and four were chosen as time points for *N*-glycan and *O*-glycan analysis as there was a significant difference in CBHI activity at those time points; with day 2 glucose culture having greater activity than day 2 lactose culture and on day 4, this relationship was reversed (Figure 10B); in addition, protein secretion, pH values and mycelial dry weight were significantly different on day 2 and not significantly different on day 4 (Figure 10A, Figure 9), offering contrasting scenarios for analysis.

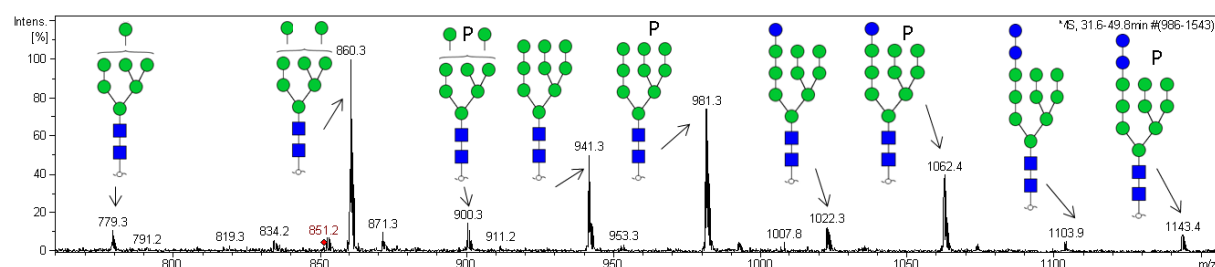


Figure 15. Summed mass spectra (Rt 32-50 min) of released *N*-glycans from total secreted proteins of RUT-C30 on day 4 of culturing with glucose as a sole carbon source. Structures shown are likely structures based on published biological pathways and previously determined *N*-glycan structure/compositions with symbol key found on page viii. Complete data tables of the retention times and corresponding possible structures can be found in the Supplementary section.

***N*-glycan analysis**

As seen in the example summed mass spectra in figure 15, and summarised for both carbon sources in figure 16 and 17, secreted protein of *T. reesei* RUT-C30 was found to possess nine different types of high-mannose *N*-glycans. In addition to differences in the number of monosaccharides, phosphorylated structures were also observed. The structures shown are those likely to correspond to the *m/z* value based on knowledge of glycosylation pathways, with composition confirmed using MS² although no linkage or monosaccharide analysis was carried out.

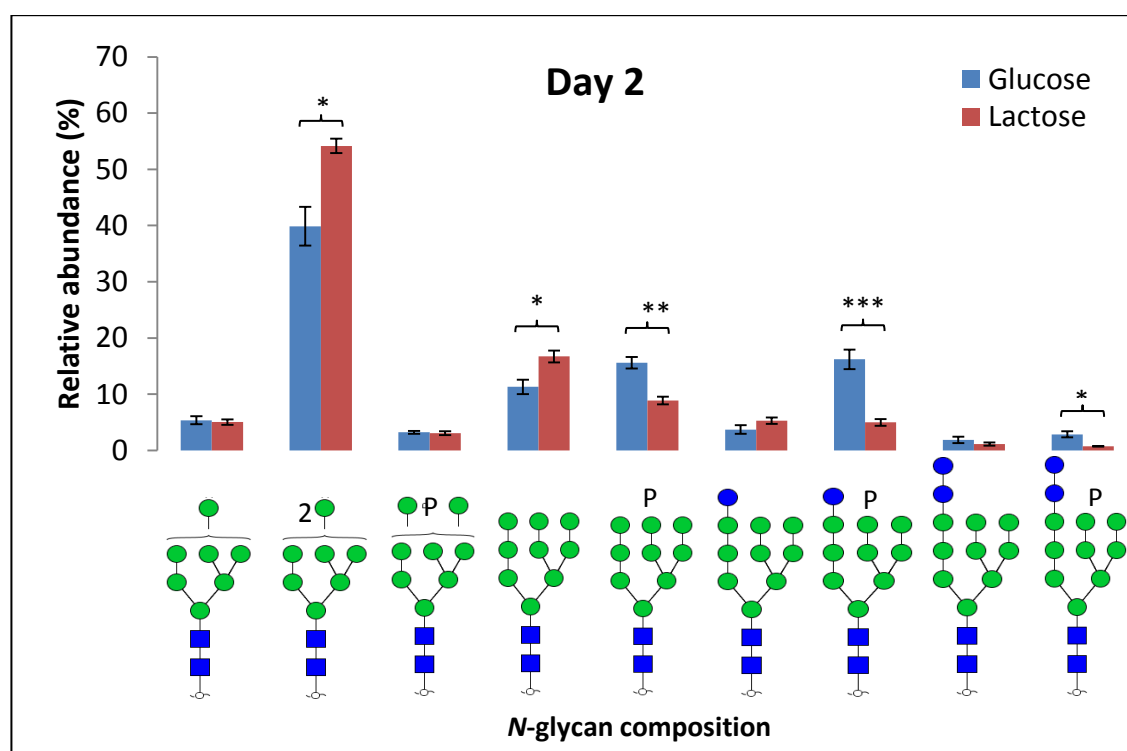


Figure 16. Relative abundances of the identified *N*-glycan compositions of RUT-C30 grown on glucose and lactose on the second day of cultivation. Hypothesised structures and compositions are based on published *N*-glycan structures and biosynthesis pathways with symbol key found on page viii. Significant differences in abundance between glucose and lactose cultures, based on three biological replicates, are indicated (*) $p < 0.05$, (**) $p < 0.01$ and (***) $p < 0.005$.

There were significant differences between secreted protein global *N*-glycosylation in glucose or lactose cultures on day 2, as shown in figure 16. The most abundant composition was found to be (Man)₈(GlcNAc)₂ with a significantly different relative abundance of 40±3% and 54±1% for glucose and lactose cultures respectively. In addition to this difference, (Man)₉(GlcNAc)₂ was produced more in lactose cultures than in glucose cultures. On the

other hand, phosphorylated and less processed glycosylated structures, $(P)_1(\text{Man})_9(\text{GlcNAc})_2$, $(P)_1(\text{Glc})_1(\text{Man})_9(\text{GlcNAc})_2$ and $(P)_1(\text{Glc})_2(\text{Man})_9(\text{GlcNAc})_2$ were significantly up-regulated in glucose cultures.

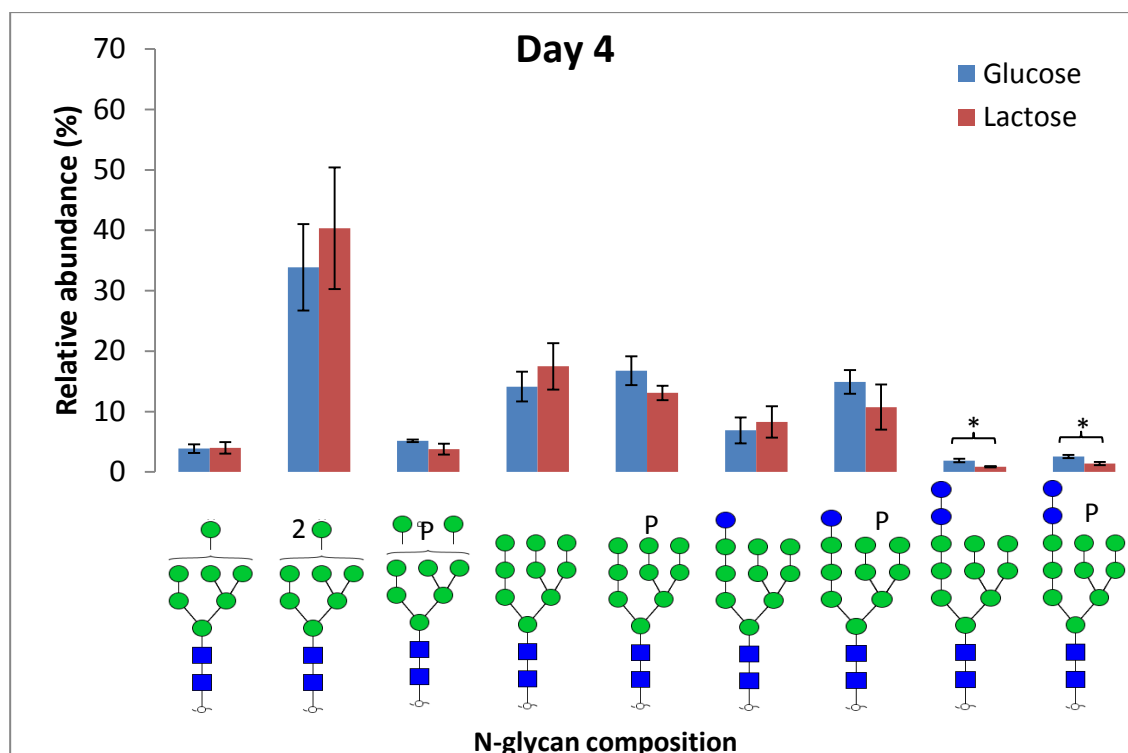


Figure 17. Relative abundances of the identified *N*-glycan compositions between growth on glucose and lactose on the fourth day of cultivation. Hypothesised structures and compositions based on published *N*-glycan structures and biosynthetic pathways with symbol key found on page viii. Significant differences in abundance between glucose and lactose cultures, based on three and two biological replicates respectively, are indicated (*) $p < 0.05$, (**) $p < 0.01$ and (***) $p < 0.005$.

N-glycan analysis of secreted protein on day 4 from glucose and lactose cultures, as shown in figure 17, revealed less of a difference in the overall *N*-glycan distribution compared to day 2 (Figure 16). Bulkier and therefore less processed *N*-glycan structures, $(\text{Glc})_2(\text{Man})_9(\text{GlcNAc})_2$ and $(P)_1(\text{Glc})_2(\text{Man})_9(\text{GlcNAc})_2$, were again found to be significantly more abundant in glucose cultures.

***O*-glycan analysis**

Secreted proteins of *T. reesei* RUT-C30 grown on glucose or lactose were found to possess five different compositions of *O*-glycans (Figure 18). The structures shown are the most abundant structures found at that mass range with composition and number of antennae confirmed using MS^2 , although no linkage or monosaccharide analysis has been performed

to confirm the exact structure. The structures shown have been chosen as they are the major structural isomers assigned to each mass based on previously published structures[36,38]. In the case of m/z values 843.3 and 1005.3, the MS^2 profile was shown to have a hexose base structure with a 176 Da moiety added with the annotated MS^2 profiles found in Supplementary section 7.4. The only monosaccharide that corresponded to the 176 Da mass was hexuronic acid (HexA), which had previously been identified in *Trichoderma reesei* in the form of the 843.3 m/z moiety[95].

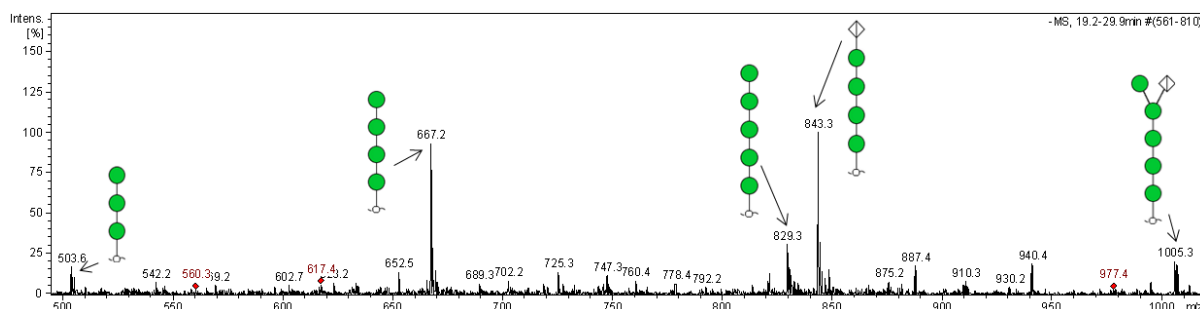


Figure 18. Summed mass spectra (Rt 19-30 min) of released *O*-glycans from secreted protein on day 2 of culturing with glucose as a sole carbon source. Structures shown are likely structures based on published biological pathways and *O*-glycan compositions, in addition to MS/MS annotation which can be found in the Supplementary section. Complete data tables of the retention times and corresponding possible structures can also be found in the Supplementary section.

As demonstrated in figure 19, structural isoforms of the same monosaccharide composition can exist for a single m/z with separation often possible using PGC-ESI- MS/MS . This example, of m/z 667.3, corresponds to an *O*-glycan composition of four mannoses, but the two separate peaks separated by PGC indicate two different isoforms of the same composition. Comparing and annotating the MS/MS spectra, using GlycoWorkBench to compute possible fragments, allows the number of antennae to be determined as well as predicting the entire structure[89]. Diagnostic structure ions, shown with stars, are unique for that structure, a useful tool for comparing similar spectra of the different isomers[38].

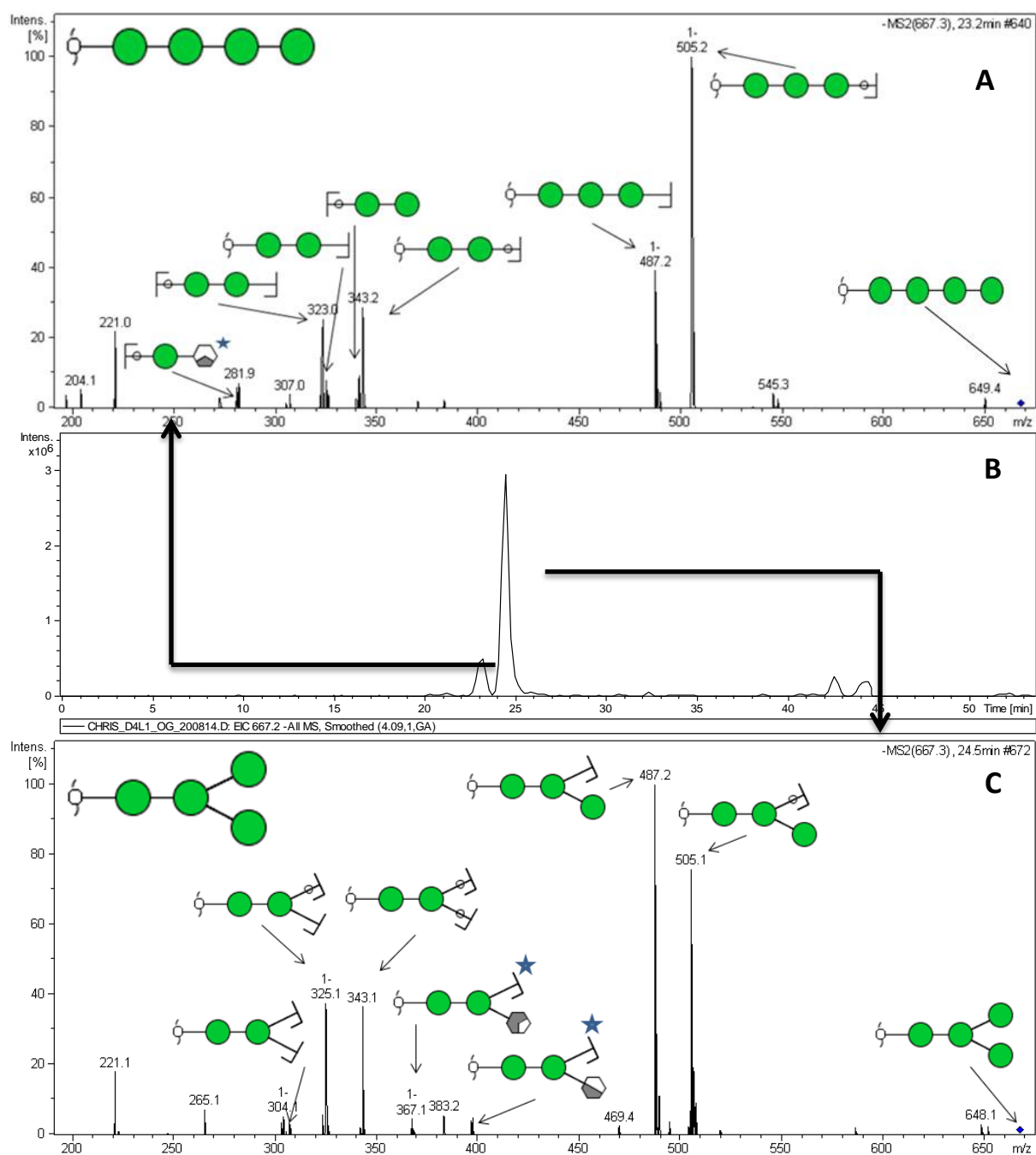


Figure 19. Identification and characterisation of *O*-glycan isomers. Negative ion fragmentation spectra of m/z 667.3 (Hex)₄ eluting at 23.2 min (a) and 24.5 min (c) are shown. (b) shows an extracted ion chromatogram of the m/z 667.3 isomers. Star denotes structural feature ions for either single antennae or double antennae structures. Monosaccharide identification based on published *O*-glycan compositions.

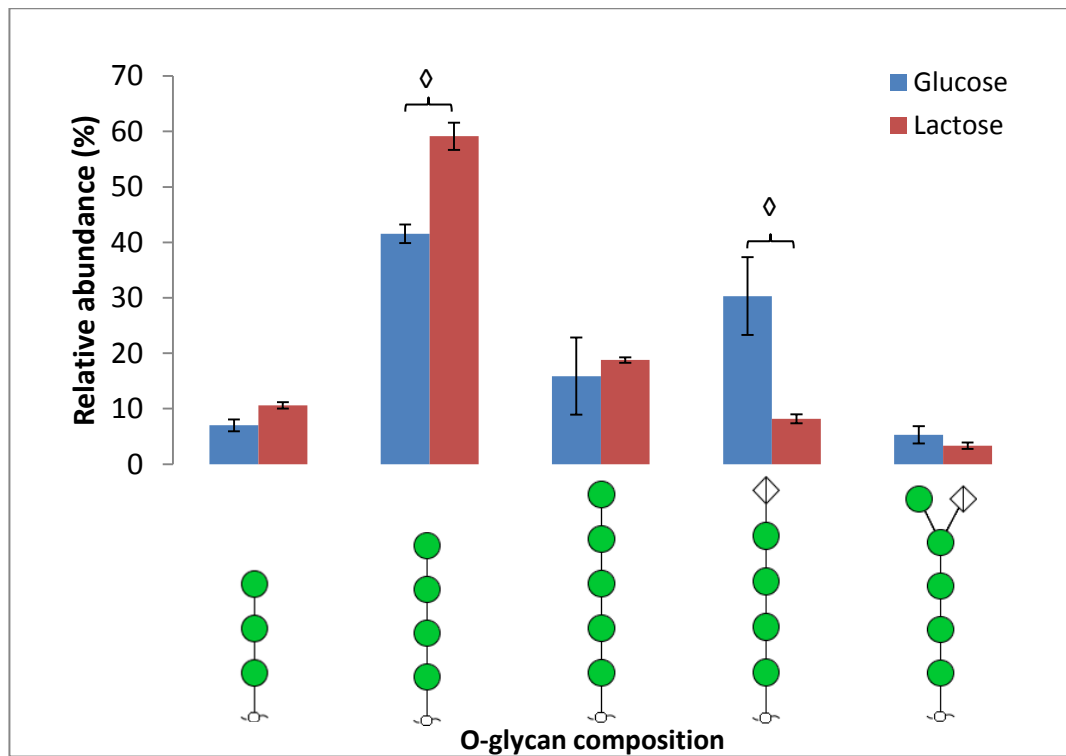


Figure 20. Relative abundances of identified *O*-glycan structures produced on total secreted proteins by growth on glucose and lactose sole carbon source cultures on the fourth day of cultivation. Number of antennae and hexose/hexuronic acid (HexA) composition determined using tandem MS annotation. Specific hexose monosaccharide determination based on previously published *O*-glycans of CBHI. Trends of low statistical significance could be observed between glucose and lactose cultures, based on biological replicates (\diamond) $p < 0.1$.

No significant difference in the *O*-glycans of RUT-C30 secreted proteins was observed on day 2 between the glucose and lactose cultures, with high variability between biological replicates observed between the relative abundances of each composition (data not shown). On day 4, the variability between biological replicates was still present so no significant differences were evident at $p < 0.05$. However, at $p < 0.1$ two structures were found to be significantly different in abundance between cultures (Figure 20). The (Hex)₄ *O*-glycan was found to be more abundant in lactose cultures while (Hex)₄(HexA)₁ was more abundant in glucose cultures. As shown in figure 21, a significant difference was observed between the relative abundance of (Hex)₃ *O*-glycan between day 2 and 4 in the lactose cultures only.

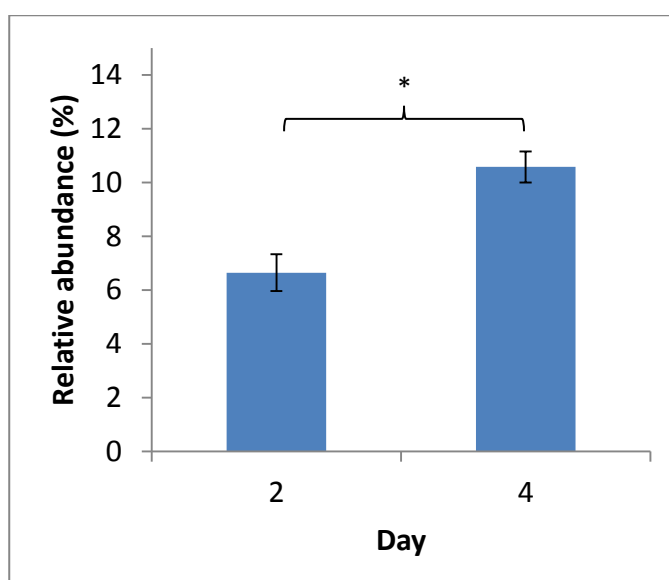


Figure 21. Relative abundances of Hex₃ O-glycan composition between day 2 and day 4 of culturing with lactose as a sole carbon source. Significant difference in relative abundance is indicated based on biological replicates (*) $p < 0.05$.

Many differences were observed when comparing the total secreted protein *N*-glycan and *O*-glycan profiles. More significant differences in the relative abundances of *N*-glycan structures between glucose and lactose cultures were found on day 2 than on day 4 (Figure 16 and figure 17). Phosphorylated *N*-glycans were found to be more abundant in secreted protein from glucose culturing compared to lactose culturing on day 2 (Figure 16). Higher variation between biological replicates was observed when analysing *O*-glycans, leading to less significantly different results between carbon sources (Figure 20). While CBHI activity was significantly different on both day 2 and day 4 between culture conditions and CBHI is said to make up most of secreted protein, no significant changes in *N*-glycan or *O*-glycan compositions could be determined to be related to this change in activity.

Chapter 4 Discussion

4.1 The value of Biolog assays for determining carbon source utilisation of *T. reesei*

The Biolog assay was used in this study as a quick screening of a large number of carbon sources for their suitability as substrates for breakdown and utilisation by *T. reesei* RUT-C30. Glucose and cellobiose (a glucose dimer) were readily utilised in the first 48 hours of growth, as were the monosaccharides mannose and *N*-acetyl glucosamine, which can be components of fungal glycans (Figure 8). However, utilisation of lactose was not detected at a statistically significant level in the 48 hour period, which was an unexpected result since lactose is known to be a nutrient source commonly used in growth media for *T. reesei* RUT-C30[96]. Two possibilities could explain why this had occurred: (i) the Biolog assay technique and associated statistical analysis were not providing an accurate indication of lactose utilisation; and/or (ii) 48 hours of incubation was not long enough for *T. reesei* to catabolise lactose to a detectable level.

Looking at the first probability, variability was relatively high between the two replicate Biolog assays used in this work, despite being prepared exactly the same way. Similarly, variability of results has been reflected in previous research involving Biolog plates [64–66]. This makes quantitative statistical analysis difficult, and low levels of carbon source utilisation can be deemed as not significantly different to the readings from water purely due to variations amongst assay replicates. In this work, this variability meant that there was no statistically significant utilisation of many common carbon sources, including lactose, in comparison to water, even though some breakdown of the indicator Tetrazolium was clearly evident in the carbon-source wells (Supplementary figure III). This suggests Biolog should be used more as a quick qualitative screening tool rather than as a high-throughput quantitative carbon source utilisation profiling tool. Moreover, as a consequence for this work, the possibility that *T. reesei* could utilise lactose during the first 48 hours of growth could not be dismissed based on the Biolog results alone.

The second possibility was that 48 hours of incubation was not long enough for *T. reesei* to catabolise lactose to a detectable level, but that more time was required by the fungus to respond with suitable enzymes to enable breakdown of the disaccharide into a more usable

form; this is in contrast to glucose, which is an immediate source of energy. The chosen incubation time was based on the work of Druzhinina *et al.*[66] which observed no significant difference in carbon utilisation profiles of *T. reesei* strains between 72 hours and 48 hours. However, neither lactose utilisation nor the strain RUT-C30 were the focus of the Druzhinina study, and a longer Biolog assay time may have been better for this work[66]. Instead, larger scale liquid cultures were used, as described in section 4.2, that showed that indeed little growth of RUT-C30 occurred on lactose until after 48 hours, after which rapid growth was observed.

In summary, the Biolog assay provided some insight into carbon source utilisation by RUT-C30, but also featured a high variability between replicates, resulting in a lack of statistical validation of trends. While this is an excellent tool for high throughput screening of carbon sources, care must be taken to only use this assay as a qualitative assay and to ensure incubation time is long enough to properly identify if carbon utilisation is possible.

4.2 Growth phases of T. reesei under different carbon sources

In order to conduct a comprehensive analysis of the effect of carbon source on growth and the glycosylation pathway of *T. reesei* RUT-C30, culturing in shake flasks was carried out using glucose and lactose as the sole carbon source. Although utilisation of lactose by RUT-C30 was not statistically validated in the Biolog assay during the first 48 hours of growth, lactose is often used successfully as a carbon source for *T. reesei* and is known to induce expression of the main secreted glycoprotein CBHI[9,97]. The catabolite-derepressed RUT-C30 strain in the presence of glucose also produces CBHI. Therefore, these two carbon sources provided a good comparative study, without the introduction of more complex insoluble carbohydrates such as cellulose (the natural *cbh1* inducer) that might interfere with downstream processing.

Measurements of pH and mycelial dry weight were conducted over four days (Figure 9). As seen in figure 9(A), mycelial growth was initially slower in the lactose culture but increased rapidly from day 3, such that there was no significant difference in mycelial weight between lactose and glucose cultures by day 4. Cultivation over a longer time period could reveal more of this trend but overall, the mycelial growth rate was consistent with literature[90,98].

The different growth patterns of RUT-C30 in the two cultures presented interesting time points for further analysis. The glucose culture rapidly entered an exponential phase of growth, which continued until day 2 but was clearly in a stationary phase by day 4. In comparison, on day 2 the lactose culture featured a lag phase and was in an exponential phase by day 4. The different phases of culture growth may have had an effect on cell physiology even when mycelial dry weight was similar between the glucose and lactose cultures at day 4. The plateauing of mycelial growth in the glucose culture may have been an indication of nutrient exhaustion or production of an inhibitory growth product [99].

The lag phase of lactose is also of interest, indicating that it takes longer for *T. reesei* to utilise lactose as a source of carbon to sustain growth, in comparison to the time required to utilise glucose, as also was evident in the Biolog assay. Extracellular hydrolysis of lactose has been identified as the main mechanism for lactose degradation by *T. reesei*, requiring the secretion of β -galactosidase, a mechanism that is co-regulated with *cbh1* induction. The β -galactosidase (Bga1) is needed to catalyse the hydrolysis of lactose to its constituent monosaccharides glucose and galactose, which can then be transported by appropriate permeases into the cell[91,100]. This mechanism could explain the pronounced lag time in growth rate for *T. reesei*, requiring the induction, expression and secretion of β -galactosidase for carbon source utilisation. In comparison, glucose readily enters the cell and provides an immediate energy supply for growth and cellular metabolism.

In addition to differences in mycelial growth, there were also differences in the pH fluctuations of the glucose and lactose cultures over the 4 day growth period. A rapid drop in pH was observed in the glucose culture at the beginning of growth until day 2 but rose again slightly by day 4. In contrast, the pH of the lactose culture slowly declined until day 4. Acidification of the culture medium, related to the rate of growth of *T. reesei* in liquid culture has been frequently documented[101–103]. The cause of this acidification has not been determined with multiple hypotheses existing to explain the mechanism including secretion of growth-associated metabolites, and a natural mechanism for improving competition against acid-vulnerable bacteria[103,104]. The pH of the medium is also known to effect the secretion and activity of extracellular enzymes. One of the secreted proteins known to have increased activity around the pH values of the cultures, 3.0-4.0, is CBHI, the main constituent of secreted protein (50-60%) by *T. reesei*.

Research has also demonstrated that maximum cellulase production occurs in the range of pH 3.0 - 5.0[105,106]. CBHI was found to be significantly more active in culture supernatant in glucose cultures than lactose cultures on day 2 and less significantly different on day 4 and this is echoed in pH values between the two cultures, suggesting a possible link. Since the pH of the glucose and lactose cultures was significantly different at day 2, and similar at day 4, these time points again presented interesting time points for subsequent metabolite and glycan analysis (Section 4.4 – 4.5).

4.3 Secreted protein concentration and CBHI activity show similar but not identical trends over the cultivation period

The concentration of secreted protein and CBHI activity were assayed to allow a subsequent analysis of any possible association with changes in the glycosylation pathway (Section 4.4 – 4.5). As protein glycosylation is essential for secretion, increased protein biosynthesis could stress this pathway. Both protein secretion and CBHI activity were greater in the glucose culture than in the lactose culture until day 3. However, on day 4 CBHI activity in the lactose culture was significantly higher than in the glucose culture despite similar extracellular protein concentrations. One likely reason for this could be the well documented inducing effect of lactose on the *cbh1* promoter, resulting in increased CBHI biosynthesis by day 4, compared to glucose which is not an inducer but simply allows CBHI expression in the catabolite de-repressed mutant RUT-C30 [96,107]. No quantitative proteomic work was performed on the culture supernatant, so detailed analysis of the relative contribution of CBHI in the total secreted protein profiles of the glucose and lactose cultures could not be made. However, SDS-PAGE and MS analysis confirmed the identity of CBHI as the main secreted protein (Supplementary section 7.5).

4.4 Analysis of nucleotides and nucleotide sugars

4.4.1 Preparation of samples for CE-UV analysis

Extraction of nucleotides and nucleotide sugars was based upon protocols used with yeast, with the one of the most commonly used extraction methods involving boiling ethanol[69]. When boiling ethanol was added to washed cells and visualised using light microscope, the cells appeared to have been disrupted and broken down. This extract was analysed with CE-UV (as per section 2.8.2), but was not found to have a detectable level of any nucleotides or

nucleotide sugars (data not shown). Another method utilised[68], chloroform:methanol:water extraction, was performed as per section 2.8.1. Cells were confirmed to be lysed and the biological extract was found to contain nucleotides and nucleotide sugars. Whilst both methods lysed the cells, nucleotides and nucleotide sugars were only found with chloroform:methanol:water extraction in this study, indicating an issue with the metabolites of interest and boiling ethanol. Villas-Boas *et al.* has rated the extraction methods and whilst the nucleotide sugar metabolite class was not investigated, nucleotides and sugars were found to be poorly extracted using boiling ethanol compared to chloroform:methanol:water[68].

As degradation was an important factor for the experimental design in this thesis, the sample preparation for biological extracts was critically evaluated. Comparing concentration methods, it was found that SpeedVac was more effective at concentrating the nucleotide standard mixture than lyophilisation. This result was surprising as freeze drying keeps the sample at cooler temperatures and in a solid phase, theoretically reducing sample degradation. The methods utilised were based on the methods applied by Villas-Boas who also found the same phenomenon of SpeedVac concentration being more effective than lyophilisation[68].

4.4.2 Nucleotide and nucleotide sugar analysis

Identification of AMP and ADP was only possible using the metabolite extraction method previously described but ATP was unable to be identified or kept stable. This was surprising as the utilised method in this thesis was very similar to a protocol described by Feng *et al.* that identified and extracted triphosphate-nucleotides. The three high energy phosphate bonds of ATP are the source of the high potential energy of this molecule. This high potential energy is also attributed to the rapid degradation of ATP making quantitation difficult in biological systems as well as standard stocks[108]. . As the standards were added to water without any buffer, as per the cited protocol, they are more likely to degrade due to a lack of metal ions to stabilise the structure. One way to reduce the spontaneous hydrolysis of ATP would be to chelate the structure with positively charged metal ions such as Mg^{2+} . If ATP was able to be identified in the cell extract, the energy status of fungi in the cell culture could have been determined using the adenylate energy charge ratio as described in the

introduction. Whilst a ratio of AMP and ADP could have been determined, ATP is essential for determining the energy state of the cell.

Ideally, the nucleotide sugars would have been quantified for their cell concentration but difficulty in standardising the number of cells collected, due to the filamentous nature of *T. reesei*, made relative abundance the best choice for quantifying the nucleotide sugars. In *T. reesei*, these selected nucleotide sugars are the precursors responsible for *N*-glycan and *O*-glycans attached to secreted proteins, in addition to other glycosylation pathways.

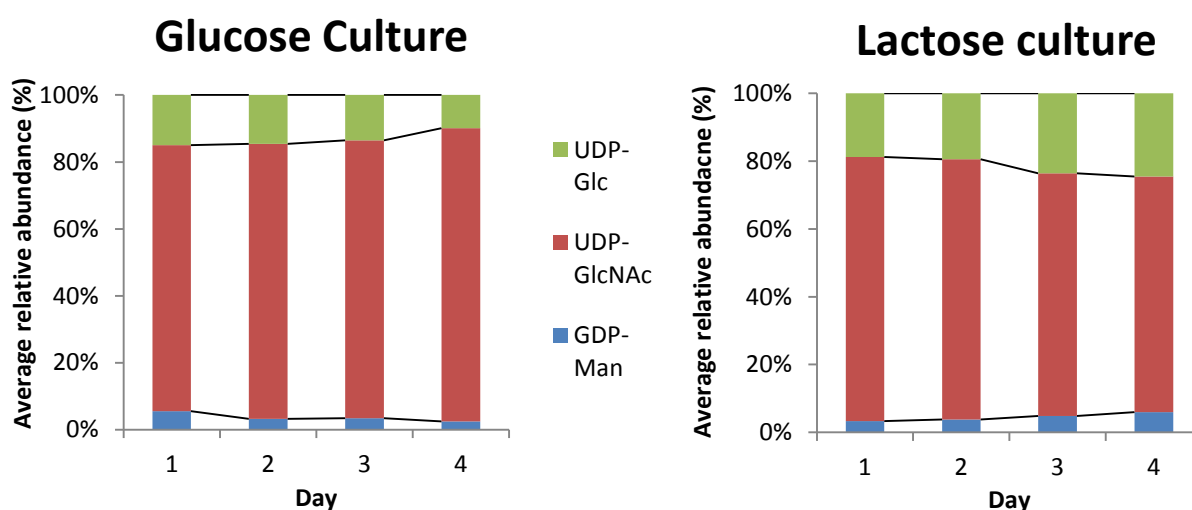


Figure 22. Overall relative abundances of intracellular nucleotide sugars in *Trichoderma reesei* RUT-C30 over four days using glucose or lactose as sole carbon sources.

Analysis of cell extracts from day 0 to day 4 was performed utilising relative abundance to measure the changes to nucleotide sugar levels inside the cell, as shown in figure 22. In the glucose culture, the relative abundance of UDP-Glc and GDP-Man decreased steadily over the duration of culture whilst UDP-GlcNAc, the major nucleotide sugar detected, increased. In the lactose culture, an opposite trend was observed with the relative abundance of UDP-GlcNAc decreasing whilst UDP-Glc and GDP-Man increased.

It is difficult to determine exactly why the abundances of these nucleotide sugars changed between carbon sources, and there was no significant change in protein glycosylation that seems to correspond to these results. Both published and investigated secreted protein glycosylation analysis revealed that mannose makes up the greatest proportion of *N*-glycans and *O*-glycans, contrasting with the distribution of nucleotide sugars with GDP-Man the lowest represented nucleotide sugar[17,21]. Two other glycosylation pathways in

filamentous fungi also utilise these nucleotide sugars, namely cell wall biosynthesis and GPI-anchor biosynthesis[54].

From the results of this thesis, it could be hypothesised that the availability of nucleotide sugars has a more significant impact on these other glycosylation processes before any impact on the secreted protein glycosylation pathway occurs. This would make sense particularly in filamentous fungi, in which the function of secreted enzymes (glycoproteins) is critical for obtaining life-sustaining nutrition from substrates such as cellulose in the environment. Monitoring of these other glycosylation pathways in addition to protein glycosylation, would form an interesting new research angle for future studies.

4.5 N-glycan and O-glycan profiles of secreted protein

Glycomic analysis by MS revealed there was no significant difference in the *N*-glycan structures from the major band identified as CBHI separated by SDS-PAGE gel and from total secreted proteins, using day 4 cultures (data not shown). As CBHI is a glycoprotein and has been documented to make up 50-60% of secreted protein of *T. reesei*, the total secreted protein glycosylation was used for *N*-glycan and *O*-glycan analysis. To focus on CBHI, one could set up a purification method for CBHI using size exclusion chromatography to obtain the purified protein and then analyse the *N*-/*O*-glycans. However, for this thesis, the overall glycan profiles for total secreted proteins were investigated as representative of the cellular glycosylation machinery as a whole.

4.5.1 The relative abundance of N-glycans in glucose and lactose cultures

Investigating the glycoproteins secreted from glucose and lactose cultures on day 2 and day 4, nine different *N*-glycan high-mannose compositions were observed, including large, glucose-capped structures that were most abundant in day 4 glucose cultures. While the specific effect of glucose and lactose as sole carbon sources in minimal media on *N*-glycans has not been investigated before for *T. reesei*, variability in the composition of the most abundant *N*-glycoforms has been observed on different media[21]. The mechanism or reason for this variability has not been fully established in filamentous fungi, although pH of the media and differential expression of secreted enzymes, including secreted glycosidases have been considered to play a role. The methods utilised in this project wouldn't be able to detect the single *N*-linked GlcNAc which had been observed by Stals *et al.*[21] as a result of

glycosidase secretion, focusing this investigation of the *N*-glycan structures larger than 300 Da.

The most abundant *N*-glycan on the secreted proteins of both glucose and lactose grown fungal cultures was (Man)₈(GlcNAc)₂ and this result was consistent with literature as the most abundant *N*-glycoform[21]. This structure was found to be more abundant in lactose cultures on day 2 compared to the glucose culture, possibly as a reflection of a lower protein secretion by RUT-C30 in the lactose cultures at that time which could indicate protein secretion stress in the glucose culture (Figure 10). In addition to this, there were more significant differences in the relative abundance of *N*-glycan structures between glucose and lactose cultures on day 2 than on day 4. This coincides with other factors such as mycelial dry weight, pH and total protein secreted that were also significantly different between cultures on day 2 but not day 4. Pinpointing the exact cause of this variation would need further experimental work to control as many variables as possible. As mentioned earlier, quantitative proteomics would be a useful complement to this work by elucidating the secreted protein profiles in each culture.

4.5.2 Phosphorylation of *N*-glycans

Phosphorylated *N*-glycans were found to be consistently more abundant on RUT-C30 secreted proteins in the glucose culture as opposed to lactose culture on day 2. As mentioned in the previous paragraph, many variables were significantly different on day 2 while not significantly different on day 4, making it difficult to determine causation but one observation was that it was more acidic in the glucose cultures compared to lactose on day 2. Phosphorylation of *N*-glycans has been previously observed in *T. reesei* RUT-C30 by Stals *et al.*[21] with the phosphate group attached to mannose. Therefore, the identity of the 80 Da moiety identified on the *N*-linked high mannose glycans on RUT-C30 secreted proteins in this thesis work was assigned as a phosphate group given that sulphate (of the same mass in ion trap MS) has not been observed on *N*-glycans in *T. reesei* to our knowledge.

While no specific role or mechanism of mannosylphosphorylation has been identified in *T. reesei* RUT-C30, more in-depth research has been performed in other fungi with particular attention on characterising the pathway and mechanism of action[33,109,110]. These *N*-glycan structures containing phosphate residues on cell wall glycoproteins have been identified to play a role in cell wall stability and formation but research into the role of these

N-glycoforms in secreted enzyme activity has not been established to our knowledge[110]. Further research into the role mannosylphosphorylation plays on *T. reesei* proteins secreted in glucose medium is required to determine a possible function.

4.5.3 The identification of extended *O*-glycan compositions

The MS analysis of the *O*-glycans attached to the secreted proteins of RUT-C30, revealed five different *O*-glycan compositions, all of which were found on secreted proteins from both glucose and lactose cultures. Two of these *O*-glycan compositions have been reported before, (Man)₃ and (Man)₄[38], attached to secreted protein of *T. reesei* and an additional one found in a related fungus species, (Man)₅[36].

One unique composition, (Hex)₅(HexA)₁ has not been previously identified although (Hex)₄(HexA)₁ has previously been identified in *T. reesei* using MS[95]. Previous research into *O*-glycans of *T. reesei* had identified (Man)₁ and (Man)₂ *O*-glycans, in addition to the observed (Man)₃ and (Man)₄ *O*-glycans, attached to CBHI peptides but these small *O*-glycans were not observed with the analytical methods used for this thesis. Focusing on *O*-glycan structure, moieties with single antennae or two antennae have been observed in this work, repeating the findings found in Christiansen *et al.*[38]. The role these *O*-glycans play has not been experimentally determined with little published on the effect of multiple antennae or length of these oligosaccharides in the fungal kingdom, rather it is believed to protect against protease action[16]. Higher variability between biological replicates was observed in these glycans compared to *N*-glycans and may be the result of tighter regulation of *N*-glycosylation compared to *O*-glycosylation[13].

4.5.4 Identification of HexA in *O*-glycans of *T. reesei*

O-glycans containing HexA produced by *T. reesei* have been reported once in genetically modified RUT-C30 but without any published confirmation using MS²[95]. MS² analysis was performed on an unusual *O*-glycan composition found on the secreted proteins of *T. reesei* in this work and a 176 Da moiety was observed, corresponding to the mass of HexA. Compositions containing this mass of HexA were found in all biological replicates thus is not likely to be contamination. Confirmation of these structures could be performed on trypsin digested glycopeptides using electron-transfer dissociation (ETD) - MS to identify the site specificity of these *O*-glycan structures. The specific acidic sugar that corresponds to the HexA mass could be glucuronic acid as it is the only synthesised nucleotide acidic sugar

shown in the *Trichoderma reesei* glycosylation pathway depicted in KEGG. If this is the case, the precursor nucleotide-sugar (likely UDP-Glucuronic acid) may be an unidentified peak in the nucleotide sugar extracts from section 3.2.

4.5.5 Role of negatively charged glycans in *T. reesei* and yeast

Whilst the biological role of HexA containing *O*-glycans has not been determined, these negatively charged *O*-glycans have been found on the secreted proteins of *T. reesei* in this work, in addition to phosphorylated *N*-glycans. The co-appearance of these monosaccharide building blocks has not been noted previously, but both share a negatively charged modification to the normally neutral glycans. Looking specifically at HexA containing *O*-glycans, the pKa of this acidic sugar has been found to be around 3-4[111]. However, as these *O*-glycans are on secreted proteins, they would be in culture medium which can reach a pH 3.0, which would result in the deprotonated form of HexA to be more abundant, making the role these acidic sugars play all the more mysterious.

Chapter 5 Summary and future directions

The overall aim of this research was to examine the effect of carbon source on the energy status and glycosylation pathways of *Trichoderma reesei* RUT-C30. High protein production and secretion, and eukaryotic glycosylation machinery make *T. reesei* RUT-C30 a suitable expression host for recombinant proteins due to its high protein production, secretion and eukaryotic glycosylation machinery. While the glycosylation of secreted proteins of RUT-C30 has been known to vary depending on culture nutrients, the impact of culture media on the intracellular precursors of glycosylation has received little attention with techniques for their analysis in fungi are lacking.

In order to investigate this, the first aim was to determine the effect of glucose and lactose on the physiological condition (growth and secreted protein) of *T. reesei*. Significant differences were observed in pH and mycelial growth between cultures using glucose and lactose as sole carbon sources, as well as secreted protein concentration and CBHI activity, mainly on days 2 and 3 of culturing. To maximise secretion of protein and highest CBHI activity, the lactose culturing conditions would be chosen. The different carbon sources had a significant effect on the physiological condition of *T. reesei*, a finding that echoes published research. The use of chemostats to culture larger volumes would be a great way to follow up on some trends of interest through the control of some variables that were not kept static in the shake flasks, such as pH or nutrients.

As nucleotide sugars had not been investigated in filamentous fungi previously, methods were developed for all stages of analysis including quenching, extraction and analysis of *T. reesei* cells in culture. This enabled investigation of the effect of carbon source on the glycosylation precursor metabolites, a relationship that had been previously unexplored. As *Trichoderma reesei* is a filamentous fungus, the number of collected cells couldn't be easily determined which caused analysis to move from absolute quantification to relative quantification. The nucleotide sugars involved in protein glycosylation were profiled, fulfilling one of the aims of the thesis, resulting in the identification of nucleotide sugar profiles over four days of culturing, with the abundances of each nucleotide sugar significantly different between the two carbon sources. The relative abundances of each nucleotide sugar (UDP-GlcNAc, GDP-Man and UDP-Glc) were found to have significantly changed over the duration of culturing. Cultures using glucose as a carbon source were found to have consistently increased the relative abundance of UDP-GlcNAc whilst cultures

using lactose as a carbon source were found to have consistently increased the relative abundance of GDP-Man and UDP-Glc.

Whilst the abundances of these nucleotide sugars changed between carbon sources, there was no significant change in protein glycosylation that seemed to correspond to these results. Two other glycosylation pathways in filamentous fungi also utilise all three of these nucleotide sugars, namely cell wall biosynthesis and GPI-anchor biosynthesis and it could be hypothesised that the availability of nucleotide sugars has a more significant impact on these other glycosylation processes before any impact on the secreted protein glycosylation pathway occurs. Monitoring of these other glycosylation pathways in addition to protein glycosylation, would form an interesting new research angle for future studies.

ATP was not able to be identified in the analysed samples due to difficulties with the stability of the standard. Through the use of buffering metal cations in future this degradation may be delayed or prevented, allowing identification of ATP and subsequent determination of the adenylate energy charge of the cultured fungi.

In this thesis, nine different compositions of *N*-glycans were identified on the produced secreted proteins of *T. reesei* RUT-C30, as well as five different *O*-glycan compositions. A few of these compositions had not been previously reported as *N*-glycans or *O*-glycans of *T. reesei* including (Hex)₅(HexA)₁. Significant differences were observed in the relative abundances of some of these compositions both between carbon sources and between culturing days, including the increased abundance of phosphorylated *N*-glycans on glucose media on the second day of culturing, although there was no obvious correlation with the changes in the nucleotide-sugar pools.

The compositional profiling of *N*-glycans and *O*-glycans of RUT-C30 secreted proteins in this thesis could be well complemented in the future by quantitative proteomic analysis of the secreted protein profiles over the four days. Site specific characterisation using glycopeptide analysis would also be interesting future research as it could determine the location of the phosphorylated *N*-glycan structures and HexA containing *O*-glycan structures, which could contribute to elucidating the role of these unusual glycans. In addition, research into the transcription and expression of enzymes involved in protein glycosylation could reveal more about the effect of carbon sources on the protein glycosylation pathway in *T. reesei* RUT-C30. Ultimately these analyses may contribute significantly to the manipulation and

enhancement of glycosylation of both endogenous and recombinant proteins in this highly utilised filamentous fungus in the future.

Chapter 6 References

- [1] Peterson, R., Nevalainen, H., *Trichoderma reesei* RUT-C30--thirty years of strain improvement. *Microbiology* 2012, 158, 58–68.
- [2] Kuhls, K., Lieckfeldt, E., Samuels, G.J., Kovacs, W., et al., Molecular evidence that the asexual industrial fungus *Trichoderma reesei* is a clonal derivative of the ascomycete *Hypocrea jecorina*. *Proc. Natl. Acad. Sci. U. S. A.* 1996, 93, 7755–60.
- [3] Mandels, M., Reese, E.T., Induction of cellulase in *Trichoderma viride* as influenced by carbon sources and metals. *J Bacteriol* 1957, 73, 269–278.
- [4] Seidl, V., Gamauf, C., Druzhinina, I.S., Seiboth, B., et al., The *Hypocrea jecorina* (*Trichoderma reesei*) hypercellulolytic mutant RUT C30 lacks a 85 kb (29 gene-encoding) region of the wild-type genome. *BMC Genomics* 2008, 9, 327.
- [5] Montenecourt, B.S., Eveleigh, D.E., Preparation of mutants of *Trichoderma reesei* with enhanced cellulase production. *Appl Env. Microbiol* 1977, 34, 777–782.
- [6] Montenecourt, B.S, Eveleigh, D. E, Selective screening methods for the isolation of high yielding cellulase mutants of *Trichoderma reesei*, 1979.
- [7] Uusitalo, J.M., Nevalainen, K.M., Harkki, a M., Knowles, J.K., Penttilä, M.E., Enzyme production by recombinant *Trichoderma reesei* strains. *J. Biotechnol.* 1991, 17, 35–49.
- [8] Kubicek, C.P., Messner, R., Gruber, F., Mach, R.L., Kubicek-Pranz, E.M., The *Trichoderma* cellulase regulatory puzzle: From the interior life of a secretory fungus. *Enzyme Microb. Technol.* 1993, 15, 90–99.
- [9] Ilmén, M., Onnela, M.L., Klemsdal, S., Keränen, S., Penttilä, M., Functional analysis of the cellobiohydrolase I promoter of the filamentous fungus *Trichoderma reesei*. *Mol. Gen. Genet.* 1996, 253, 303–314.
- [10] Nakari-Setälä, T., Paloheimo, M., Kallio, J., Vehmaanperä, J., et al., Genetic modification of carbon catabolite repression in *Trichoderma reesei* for improved protein production. *Appl. Environ. Microbiol.* 2009, 75, 4853–60.
- [11] Nevalainen, K.M.H., Te’o, V.S.J., Bergquist, P.L., Heterologous protein expression in filamentous fungi. *Trends Biotechnol.* 2005, 23, 468–474.
- [12] Goldberg, A.L., Protein degradation and protection against misfolded or damaged proteins. *Nature* 2003, 426, 895–899.
- [13] Ajit Varki Jeffrey Esko, Hudson Freeze, Gerald Hart, Jamey Marth, R.C., *Essentials of Glycobiology*, vol. 1, 1999.

- [14] Salovuori, I., Makarow, M., Rauvala, H., Knowles, J., Kääriäinen, L., Low Molecular Weight High-Mannose Type Glycans in a Secreted Protein of the Filamentous Fungus *Trichoderma Reesei*. *Nat. Biotechnol.* 1987, 5, 152–156.
- [15] Roth, J., Zuber, C., Park, S., Jang, I., et al., Protein N-glycosylation, protein folding, and protein quality control. *Mol. Cells* 2010, 30, 497–506.
- [16] Beckham, G.T., Dai, Z., Matthews, J.F., Momany, M., et al., Harnessing glycosylation to improve cellulase activity. *Curr. Opin. Biotechnol.* 2012, 23, 338–45.
- [17] Stals, I., Sandra, K., Devreese, B., Van Beeumen, J., Claeysens, M., Factors influencing glycosylation of *Trichoderma reesei* cellulases. II: N-glycosylation of Cel7A core protein isolated from different strains. *Glycobiology* 2004, 14, 725–37.
- [18] Maras, M., De Bruyn, A., Vervecken, W., Uusitalo, J., et al., In vivo synthesis of complex N-glycans by expression of human N-acetylglucosaminyltransferase I in the filamentous fungus *Trichoderma reesei*. *FEBS Lett.* 1999, 452, 365–370.
- [19] Klarskov, K., Piens, K., Stahlberg, J., Haaj, P.B., et al., Cellobiohydrolase I from *Trichoderma reesei*: Identification of an active-site nucleophile and additional information on sequence including the glycosylation pattern of the core protein. *Carbohydr. Res.* 1997, 304, 143–154.
- [20] Harrison, M.J., Nouwens, A.S., Jardine, D.R., Zachara, N.E., et al., Modified glycosylation of cellobiohydrolase I from a high cellulase-producing mutant strain of *Trichoderma reesei*. *Eur. J. Biochem.* 1998, 256, 119–127.
- [21] Stals, I., Sandra, K., Geysens, S., Contreras, R., et al., Factors influencing glycosylation of *Trichoderma reesei* cellulases. I: Postsecretorial changes of the O- and N-glycosylation pattern of Cel7A. *Glycobiology* 2004, 14, 713–24.
- [22] Lehle, L., Strahl, S., Tanner, W., Protein glycosylation, conserved from yeast to man: A model organism helps elucidate congenital human diseases. *Angew. Chemie - Int. Ed.* 2006, 45, 6802–6818.
- [23] Edwards, M., Endo-Beta-N-Acetylglucosaminidase Enzymes Secreted by *T. Reesei*. 2008.
- [24] Shoemaker, S., Watt, K., Tsitovsky, G., Cox, R., Characterization and Properties of Cellulases Purified from *Trichoderma Reesei* Strain L27. *Bio/Technology* 1983, 1, 687–690.
- [25] Foreman, P.K., Brown, D., Dankmeyer, L., Dean, R., et al., Transcriptional regulation of biomass-degrading enzymes in the filamentous fungus *Trichoderma reesei*. *J. Biol. Chem.* 2003, 278, 31988–31997.
- [26] Chen, C., Gritzali, M., Stafford, D., Nucleotide Sequence and Deduced Primary Structure of Cellobiohydrolase II from *Trichoderma Reesei*. *Nat. Biotechnol.* 1987, 5, 274 – 278.
- [27] Penttilä, M., Nevalainen, H., Rättö, M., Salminen, E., Knowles, J., A versatile transformation system for the cellulolytic filamentous fungus *Trichoderma reesei*. *Gene* 1987, 61, 155–164.

- [28] Saloheimo, M., Lehtovaara, P., Penttilä, M., Teeri, T.T., et al., EGIII, a new endoglucanase from *Trichoderma reesei*: the characterization of both gene and enzyme. *Gene* 1988, 63, 11–22.
- [29] Kollmann, K., Pohl, S., Marschner, K., Encarnação, M., et al., Mannose phosphorylation in health and disease. *Eur. J. Cell Biol.* 2010, 89, 117–123.
- [30] Barnes, J., Lim, J.M., Godard, A., Blanchard, F., et al., Extensive mannose phosphorylation on leukemia inhibitory factor (LIF) controls its extracellular levels by multiple mechanisms. *J. Biol. Chem.* 2011, 286, 24855–24864.
- [31] Pohl, S., Marschner, K., Storch, S., Bräulke, T., Glycosylation- and phosphorylation-dependent intracellular transport of lysosomal hydrolases. *Biol. Chem.* 2009, 390, 521–527.
- [32] Hui, J.P.M., White, T.C., Thibault, P., Identification of glycan structure and glycosylation sites in cellobiohydrolase II and endoglucanases I and II from *Trichoderma reesei*. *Glycobiology* 2002, 12, 837–849.
- [33] Jigami, Y., Odani, T., Mannosylphosphate transfer to yeast mannan. *Biochim. Biophys. Acta - Gen. Subj.* 1999, 1426, 335–345.
- [34] Kukuruzinska, M.A., Lennon, K., Growth-related coordinate regulation of the early *N*-glycosylation genes in yeast. *Glycobiology* 1994, 4, 437–443.
- [35] Goto, M., Protein *O*-glycosylation in fungi: diverse structures and multiple functions. *Biosci. Biotechnol. Biochem.* 2007, 71, 1415–1427.
- [36] Goto, M., Tsukamoto, M., Kwon, I., Ekino, K., Furukawa, K., Functional analysis of *O*-linked oligosaccharides in threonine/serine-rich region of *Aspergillus glucoamylase* by expression in mannosyltransferase-disruptants of yeast. *Eur. J. Biochem.* 1999, 260, 596–602.
- [37] Zakrzewska, A., Migdalski, A., Saloheimo, M., Penttilä, M.E., et al., cDNA encoding protein *O*-mannosyltransferase from the filamentous fungus *Trichoderma reesei*; functional equivalence to *Saccharomyces cerevisiae* PMT2. *Curr Genet* 2003, 43, 11–16.
- [38] Christiansen, M.N., Kolarich, D., Nevalainen, H., Packer, N.H., Jensen, P.H., Challenges of determining *O*-glycopeptide heterogeneity: a fungal glucanase model system. *Anal. Chem.* 2010, 82, 3500–9.
- [39] Hayter, P.M., Curling, E.M.A., Baines, A.J., Jenkins, N., et al., Glucose-Limited Chemostat Culture of Chinese Hamster Ovary Cells Producing Recombinant Human Interferon- γ . *Biotechnol. Bioeng.* 1992, 39, 327–335.
- [40] Barnabé, N., Butler, M., The effect of glucose and glutamine on the intracellular nucleotide pool and oxygen uptake rate of a murine hybridoma. *Cytotechnology* 2000, 34, 47–57.
- [41] Borys, M.C., Linzer, D.I., Papoutsakis, E.T., Culture pH affects expression rates and glycosylation of recombinant mouse placental lactogen proteins by Chinese hamster ovary (CHO) cells. *Biotechnology. (N. Y.)* 1993, 11, 720–724.

- [42] Kochanowski, N., Blanchard, F., Cacan, R., Chirat, F., et al., Influence of intracellular nucleotide and nucleotide sugar contents on recombinant interferon-gamma glycosylation during batch and fed-batch cultures of CHO cells. *Biotechnol. Bioeng.* 2008, 100, 721–33.
- [43] Idle, J.R., Gonzalez, F.J., Metabolomics. *Cell Metab.* 2007, 6, 348–351.
- [44] Zhu, J., Sova, P., Xu, Q., Dombek, K.M., et al., Stitching together multiple data dimensions reveals interacting metabolomic and transcriptomic networks that modulate cell regulation. *PLoS Biol.* 2012, 10.
- [45] Kaddurah-Daouk, R., Kristal, B.S., Weinshilboum, R.M., Metabolomics: a global biochemical approach to drug response and disease. *Annu. Rev. Pharmacol. Toxicol.* 2008, 48, 653–683.
- [46] Studier, F.W., Protein production by auto-induction in high-density shaking cultures. *Protein Expr. Purif.* 2005, 41, 207–234.
- [47] Dietmair, S., Timmins, N.E., Gray, P.P., Nielsen, L.K., Krömer, J.O., Towards quantitative metabolomics of mammalian cells: development of a metabolite extraction protocol. *Anal. Biochem.* 2010, 404, 155–164.
- [48] Jannasch, A., Sedlak, M., Adamec, J., Metabolic Profiling 2011, 708, 159–171.
- [49] Lu, W., Bennett, B.D., Rabinowitz, J.D., Analytical strategies for LC-MS-based targeted metabolomics. *J. Chromatogr. B. Analyt. Technol. Biomed. Life Sci.* 2008, 871, 236–42.
- [50] Griffiths, W.J., Koal, T., Wang, Y., Kohl, M., et al., Targeted metabolomics for biomarker discovery. *Angew. Chem. Int. Ed. Engl.* 2010, 49, 5426–5445.
- [51] Adamski, J., Suhre, K., Metabolomics platforms for genome wide association studies-linking the genome to the metabolome. *Curr. Opin. Biotechnol.* 2013, 24, 39–47.
- [52] Hirschberg, C.B., Robbins, P.W., Abeijon, C., Transporters of nucleotide sugars, ATP, and nucleotide sulfate in the endoplasmic reticulum and Golgi apparatus. *Annu. Rev. Biochem.* 1998, 67, 49–69.
- [53] Lunt, S.Y., Vander Heiden, M.G., Aerobic Glycolysis: Meeting the Metabolic Requirements of Cell Proliferation. *Annu. Rev. Cell Dev. Biol.* 2011, 27, 441–464.
- [54] Ogata, H., Goto, S., Sato, K., Fujibuchi, W., et al., KEGG: Kyoto encyclopedia of genes and genomes. *Nucleic Acids Res.* 1999, 27, 29–34.
- [55] Harvey, D.J., Fragmentation of negative ions from carbohydrates: Part 2. Fragmentation of high-mannose *N*-linked glycans. *J. Am. Soc. Mass Spectrom.* 2005, 16, 631–646.
- [56] Deshpande, N., Wilkins, M.R., Packer, N., Nevalainen, H., Protein glycosylation pathways in filamentous fungi. *Glycobiology* 2008, 18, 626–37.
- [57] Kochanowski, N., Blanchard, F., Cacan, R., Chirat, F., et al., Intracellular nucleotide and nucleotide sugar contents of cultured CHO cells determined by a fast, sensitive, and high-resolution ion-pair RP-HPLC. *Anal. Biochem.* 2006, 348, 243–251.

- [58] Gibeaut, D.M., Nucleotide sugars and glycosyltransferases for synthesis of cell wall matrix polysaccharides. *Plant Physiol. Biochem.* 2000, 38, 69–80.
- [59] Costas, C., Yuriev, E., Meyer, K.L., Guion, T.S., Hanna, M.M., RNA-protein crosslinking to AMP residues at internal positions in RNA with a new photocrosslinking ATP analog. *Nucleic Acids Res.* 2000, 28, 1849–1858.
- [60] Sklar, F.H., McKee, K.L., Adenylate energy charge (AEC) response to stress and extraction technique in the Louisiana swamp crayfish, *Procambarus clarkii*. *Bull. Environ. Contam. Toxicol.* 1984, 33, 584–591.
- [61] Gajewski, E., Steckler, D.K., Goldberg, R.N., Thermodynamics of the hydrolysis of adenosine 5'-triphosphate to adenosine 5'-diphosphate. *J. Biol. Chem.* 1986, 261, 12733–12737.
- [62] Mashego, M.R., Rumbold, K., De Mey, M., Vandamme, E., et al., Microbial metabolomics: past, present and future methodologies. *Biotechnol. Lett.* 2007, 29, 1–16.
- [63] Shea, A., Wolcott, M., Daefler, S., Rozak, D.A., Biolog phenotype microarrays. *Methods Mol. Biol.* 2012, 881, 331–373.
- [64] Stefanowicz, A., The biolog plates technique as a tool in ecological studies of microbial communities. *Polish J. Environ. Stud.* 2006, 15, 669–676.
- [65] Singh, M.P., Application of Biolog FF MicroPlate for substrate utilization and metabolite profiling of closely related fungi. *J. Microbiol. Methods* 2009, 77, 102–108.
- [66] Druzhinina, I.S., Schmoll, M., Seiboth, B., Kubicek, C.P., Global carbon utilization profiles of wild-type, mutant, and transformant strains of *Hypocrea jecorina*. *Appl. Environ. Microbiol.* 2006, 72, 2126–33.
- [67] Nasution, U., Gulik, W.M. Van, Kleijn, R.J., Winden, W.A. Van, Measurement of Intracellular Metabolites of Primary Metabolism and Adenine Nucleotides in Chemostat Cultivated *Penicillium chrysogenum* 2006.
- [68] Villas-Bôas, S.G., Højer-Pedersen, J., Åkesson, M., Smedsgaard, J., Nielsen, J., Global metabolite analysis of yeast: Evaluation of sample preparation methods. *Yeast* 2005, 22, 1155–1169.
- [69] Gonzalez, B., François, J., Renaud, M., A rapid and reliable method for metabolite extraction in yeast using boiling buffered ethanol. *Yeast* 1997, 13, 1347–1355.
- [70] Shihabi, Z.K., in: *J. Chromatogr. A*, vol. 1027, 2004, pp. 179–184.
- [71] Rabinä, J., Mäki, M., Savilahti, E.M., Järvinen, N., et al., Analysis of nucleotide sugars from cell lysates by ion-pair solid-phase extraction and reversed-phase high-performance liquid chromatography. *Glycoconj. J.* 2001, 18, 799–805.

- [72] Feng, H.-T., Wong, N., Wee, S., Lee, M.M., Simultaneous determination of 19 intracellular nucleotides and nucleotide sugars in Chinese Hamster ovary cells by capillary electrophoresis. *J. Chromatogr. B. Analyt. Technol. Biomed. Life Sci.* 2008, 870, 131–4.
- [73] Wätzig, H., Degenhardt, M., Kunkel, A., Strategies for capillary electrophoresis: method development and validation for pharmaceutical and biological applications. *Electrophoresis* 1998, 19, 2695–2752.
- [74] Mariño, K., Bones, J., Kattla, J.J., Rudd, P.M., A systematic approach to protein glycosylation analysis: a path through the maze. *Nat. Chem. Biol.* 2010, 6, 713–723.
- [75] Jensen, P.H., Karlsson, N.G., Kolarich, D., Packer, N.H., Structural analysis of *N*- and *O*-glycans released from glycoproteins. *Nat. Protoc.* 2012, 7, 1299–1310.
- [76] Stadlmann, J., Pabst, M., Kolarich, D., Kunert, R., Altmann, F., Analysis of immunoglobulin glycosylation by LC-ESI-MS of glycopeptides and oligosaccharides. *Proteomics* 2008, 8, 2858–2871.
- [77] Pabst, M., Altmann, F., Influence of electrosorption, solvent, temperature, and ion polarity on the performance of LC-ESI-MS using graphitic carbon for acidic oligosaccharides. *Anal. Chem.* 2008, 80, 7534–7542.
- [78] Everest-Dass, A. V., Abrahams, J.L., Kolarich, D., Packer, N.H., Campbell, M.P., Structural feature ions for distinguishing *N*- and *O*-linked glycan isomers by LC-ESI-IT MS/MS. *J. Am. Soc. Mass Spectrom.* 2013, 24, 895–906.
- [79] Kolarich, D., Jensen, P.H., Altmann, F., Packer, N.H., Determination of site-specific glycan heterogeneity on glycoproteins. *Nat. Protoc.* 2012, 7, 1285–1298.
- [80] Forgács, E., Cserháti, T., Relationship between retention characteristics and physicochemical parameters of solutes on porous graphitized carbon column. *J. Pharm. Biomed. Anal.* 1998, 18, 505–510.
- [81] Pabst, M., Bondili, J.S., Stadlmann, J., Mach, L., Altmann, F., Mass + retention time = structure: A strategy for the analysis of *N*-glycans by carbon LC-ESI-MS and its application to fibrin *N*-glycans. *Anal. Chem.* 2007, 79, 5051–5057.
- [82] Eveleigh, D.E., Montenecourt, B.S., Increasing yields of extracellular enzymes. *Adv Appl Microbiol* 1979, 25, 57–74.
- [83] Kubicek, C.P., Microbiology and Biotechnology Release of Carboxymethyl-Cellulase and *B*-Glucosidase from Cell Walls of *Trichoderma reesei*. *Eur. J. Appl. Microbiol. Biotechnol.* 1981, 13, 226–231.
- [84] Nanodrop, P., Bradford Protein Assay. *Methods* 1976, 2003, 1–4.
- [85] De Koning, W., van Dam, K., A method for the determination of changes of glycolytic metabolites in yeast on a subsecond time scale using extraction at neutral pH. *Anal. Biochem.* 1992, 204, 118–123.

- [86] Laemmli, U.K., Cleavage of structural proteins during the assembly of the head of bacteriophage T4. *Nature* 1970, 227, 680–685.
- [87] Royle, L., Radcliffe, C.M., Dwek, R.A., Rudd, P.M., Detailed structural analysis of *N*-glycans released from glycoproteins in SDS-PAGE gel bands using HPLC combined with exoglycosidase array digestions. *Methods Mol. Biol.* 2006, 347, 125–143.
- [88] Cooper, C.A., Gasteiger, E., Packer, N.H., GlycoMod--a software tool for determining glycosylation compositions from mass spectrometric data. *Proteomics* 2001, 1, 340–349.
- [89] Ceroni, A., Maass, K., Geyer, H., Geyer, R., et al., GlycoWorkbench: A tool for the computer-assisted annotation of mass spectra of glycans. *J. Proteome Res.* 2008, 7, 1650–1659.
- [90] Pakula, T.M., Salonen, K., Uusitalo, J., Penttilä, M., The effect of specific growth rate on protein synthesis and secretion in the filamentous fungus *Trichoderma reesei*. *Microbiology* 2005, 151, 135–43.
- [91] Ivanova, C., Bååth, J. a, Seiboth, B., Kubicek, C.P., Systems analysis of lactose metabolism in *Trichoderma reesei* identifies a lactose permease that is essential for cellulase induction. *PLoS One* 2013, 8, e62631.
- [92] Collén, A., Saloheimo, M., Bailey, M., Penttilä, M., Pakula, T.M., Protein production and induction of the unfolded protein response in *Trichoderma reesei* strain Rut-C30 and its transformant expressing endoglucanase I with a hydrophobic tag. *Biotechnol. Bioeng.* 2005, 89, 335–344.
- [93] Juhász, T., Szengyel, Z., Sziártó, N., Réczey, K., Effect of pH on cellulase production of *Trichoderma reesei* RUT C30. *Appl. Biochem. Biotechnol.* 2004, 113-116, 201–11.
- [94] Grimm, L.H., Kelly, S., Krull, R., Hempel, D.C., Morphology and productivity of filamentous fungi. *Appl. Microbiol. Biotechnol.* 2005, 69, 375–384.
- [95] Miyauchi, S., Te’o, V.S., Bergquist, P.L., Nevalainen, K.M.H., Expression of a bacterial xylanase in *Trichoderma reesei* under the *egl2* and *cbh2* glycosyl hydrolase gene promoters. *N. Biotechnol.* 2013, 30, 523–30.
- [96] Dashtban, M., Buchkowski, R., Qin, W., Effect of different carbon sources on cellulase production by *Hypocrea jecorina* (*Trichoderma reesei*) strains. *Int. J. Biochem. Mol. Biol.* 2011, 2, 274–86.
- [97] Pakula, T.M., Uusitalo, J., Saloheimo, M., Salonen, K., et al., Monitoring the kinetics of glycoprotein synthesis and secretion in the filamentous fungus *Trichoderma reesei*: Cellobiohydrolase I (CBHI) as a model protein. *Microbiology* 2000, 146, 223–232.
- [98] Olsson, L., Christensen, T.M.I.E., Hansen, K.P., Palmqvist, E.A., Influence of the carbon source on production of cellulases, hemicellulases and pectinases by *Trichoderma reesei* Rut C-30. *Enzyme Microb. Technol.* 2003, 33, 612–619.
- [99] Herman, P.K., Stationary phase in yeast. *Curr. Opin. Microbiol.* 2002, 5, 602–607.

- [100] Seiboth, B., Pakdaman, B.S., Hartl, L., Kubicek, C.P., Lactose metabolism in filamentous fungi: how to deal with an unknown substrate. *Fungal Biol. Rev.* 2007, 21, 42–48.
- [101] Rosling, A., Lindahl, B.D., Taylor, A.F.S., Finlay, R.D., Mycelial growth and substrate acidification of ectomycorrhizal fungi in response to different minerals. *FEMS Microbiol. Ecol.* 2004, 47, 31–37.
- [102] Murakami, C.J., Wall, V., Basisty, N., Kaeberlein, M., Composition and acidification of the culture medium influences chronological aging similarly in vineyard and laboratory yeast. *PLoS One* 2011, 6.
- [103] Schmoll, M., Schuster, A., Biology and biotechnology of *Trichoderma*. *Appl. Microbiol. Biotechnol.* 2010, 87, 787–799.
- [104] Kredics, L., Antal, Z., Szekeres, A., Hatvani, L., et al., Extracellular proteases of *Trichoderma* species. A review. *Acta Microbiol. Immunol. Hung.* 2005, 52, 169–184.
- [105] Li, C., Yang, Z., Zhang, R.H.C., Zhang, D., et al., Effect of pH on cellulase production and morphology of *Trichoderma reesei* and the application in cellulosic material hydrolysis. *J. Biotechnol.* 2013, 168, 470–7.
- [106] Juhász, T., Szengyel, Z., Szijártó, N., Réczey, K., Effect of pH on cellulase production of *Trichoderma reesei* RUT C30. *Appl. Biochem. Biotechnol.* 2004, 113-116, 201–211.
- [107] Pakula, T.M., Uusitalo, J., Saloheimo, M., Salonen, K., et al., Monitoring the kinetics of glycoprotein synthesis and secretion in the filamentous fungus *Trichoderma reesei*: cellobiohydrolase I (CBHI) as a model protein. *Microbiology* 2000, 146 (Pt 1, 223–32.
- [108] Heyn, M.P., Bretz, R., The self association of ATP: thermodynamics and geometry. *Biophys. Chem.* 1975, 3, 35–45.
- [109] Conde, R., Pablo, G., Cueva, R., Larriba, G., Screening for new yeast mutants affected in mannosylphosphorylation of cell wall mannoproteins. *Yeast* 2003, 20, 1189–1211.
- [110] Hazen, K.C., Singleton, D.R., Masuoka, J., Influence of outer region mannosylphosphorylation on N-glycan formation by *Candida albicans*: Normal acid-stable N-glycan formation requires acid-labile mannosylphosphate addition. *Glycobiology* 2007, 17, 1052–1060.
- [111] Wang, H.M., Loganathan, D., Linhardt, R.J., Determination of the pKa of glucuronic acid and the carboxy groups of heparin by ¹³C-nuclear-magnetic-resonance spectroscopy. *Biochem. J.* 1991, 278 (Pt 3, 689–695.

Chapter 7 Supplementary Material

7.1 Biolog

26270	26959	21266	43053	23197	39257	29751	23571	30532	44142	42398	39037
21677	21999	28326	28445	32580	26391	29842	12983	35476	28090	31592	38024
35024	21370	28391	41739	32133	23921	39597	28391	24662	22099	23384	23746
40830	35407	24533	27761	25343	25311	24263	30574	23572	26072	24701	26771
35010	33741	22305	38304	31701	27364	27001	26923	38160	33204	32584	33415
38772	15464	29809	18653	32392	24878	35462	29126	26672	29138	34267	38686
23806	18685	19017	33410	24584	24833	32457	41423	36020	39322	41056	42808
37935	39360	34610	34271	36377	35125	29595	21485	29971	32167	30590	29479

Figure I. Area values demonstrating utilisation of each carbon source after 48 hours of incubation at 28°C featuring a heat map with low usage as red and high usage as green.

Water	Tween 80	N-acetyl-D-Galactosamine	N-acetyl-D-Glucosamine	N-acetyl-D-Mannosamine	Adonitol	Amygdalin	D-Arabinose	L-Arabinose	D-Arabitol	Arbutin	D-Cellobiose
α -Cyclodextrin	β -Cyclodextrin	Dextrin	i-Erythritol	D-Fructose	L-Fucose	D-Galactose	D-Galcturonic Acid	Gentiobiose	D-Gluconic Acid	D-Glucosamine	α -D-Glucose
Glucose-1-Phosphate	Glucuronamide	D-Glucuronic Acid	Glycerol	Glycogen	m-Inositol	2-Keto-D-Gluconic Acid	α -D-Lactose	Lactulose	Maltitol	Maltose	Maltotriose
D-Mannitol	D-Mannose	D-Melezitose	D-Melibiose	α -Methyl-D-Galactoside	β -Methyl-D-Galactoside	α -Methyl-D-Glucoside	β -Methyl-D-Glucoside	Palatinose	D-Psicose	D-Raffinose	L-Rhamnose
D-Ribose	Salicin	Sedoheptulosan	D-Sorbitol	L-Sorbose	Stachyose	Sucrose	D-Tagatose	D-Trehalose	Turanose	Xylitol	D-Xylose
γ -Amino-butyric Acid	Bromosuccinic Acid	Fumaric Acid	β -Hydroxy-butyric Acid	γ -Hydroxy-butyric Acid	p-Hydroxyphenyl-acetic Acid	α -Keto-glutaric Acid	D-Lactic Acid Methyl Ester	L-Lactic Acid	D-Malic Acid	L-Malic Acid	Quinic Acid
D-Saccharic Acid	Sebacic Acid	Succinamic Acid	Succinic Acid	Succinic Acid Mono-methyl ester	N-Acetyl-L-Glutamic Acid	Alaninamide	L-Alanine	L-Alanyl-Glycine	L-Asparagine	L-Aspartic Acid	L-Glutamic Acid
Glycyl-L-Glutamic Acid	L-Ornithine	L-Phenylalanine	L-Proline	L-Pyrogutamic Acid	L-Serine	L-Threonine	2-Amino Ethanol	Putrescine	Adenosine	Uridine	AMP

Figure II. Carbon sources for each well featuring the same heat map as figure 1.

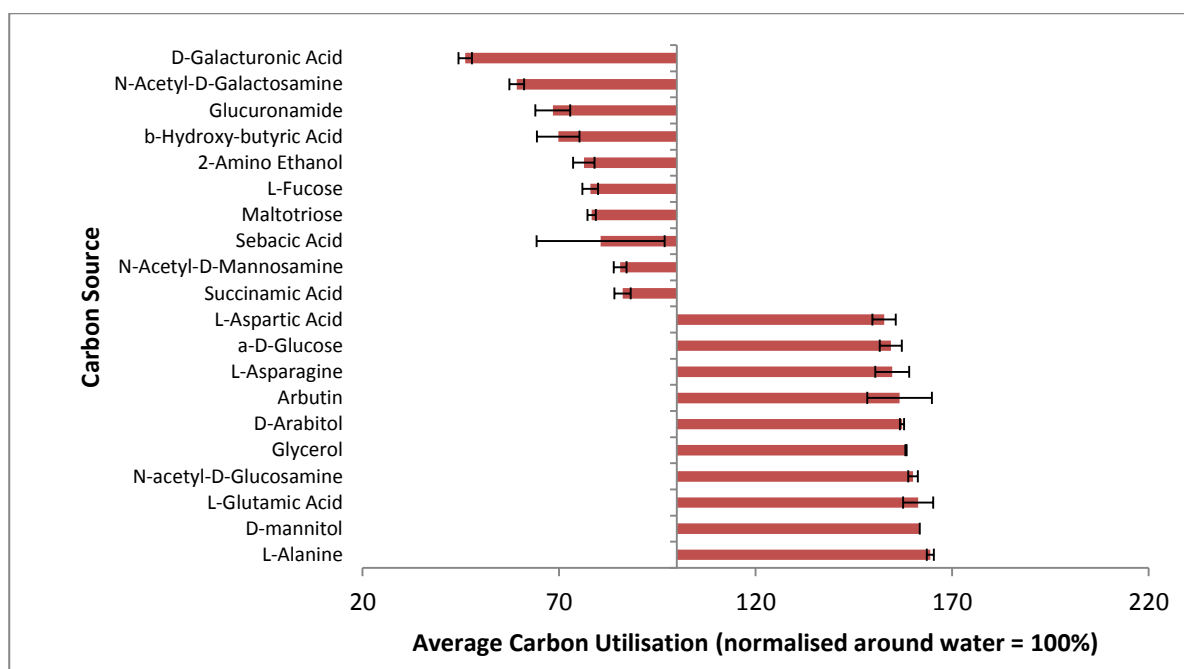


Figure III. Top 10 and bottom 10 carbon sources with areas normalised around water with two biological replicates.

7.2 Capillary electrophoresis peak allocation procedure and data

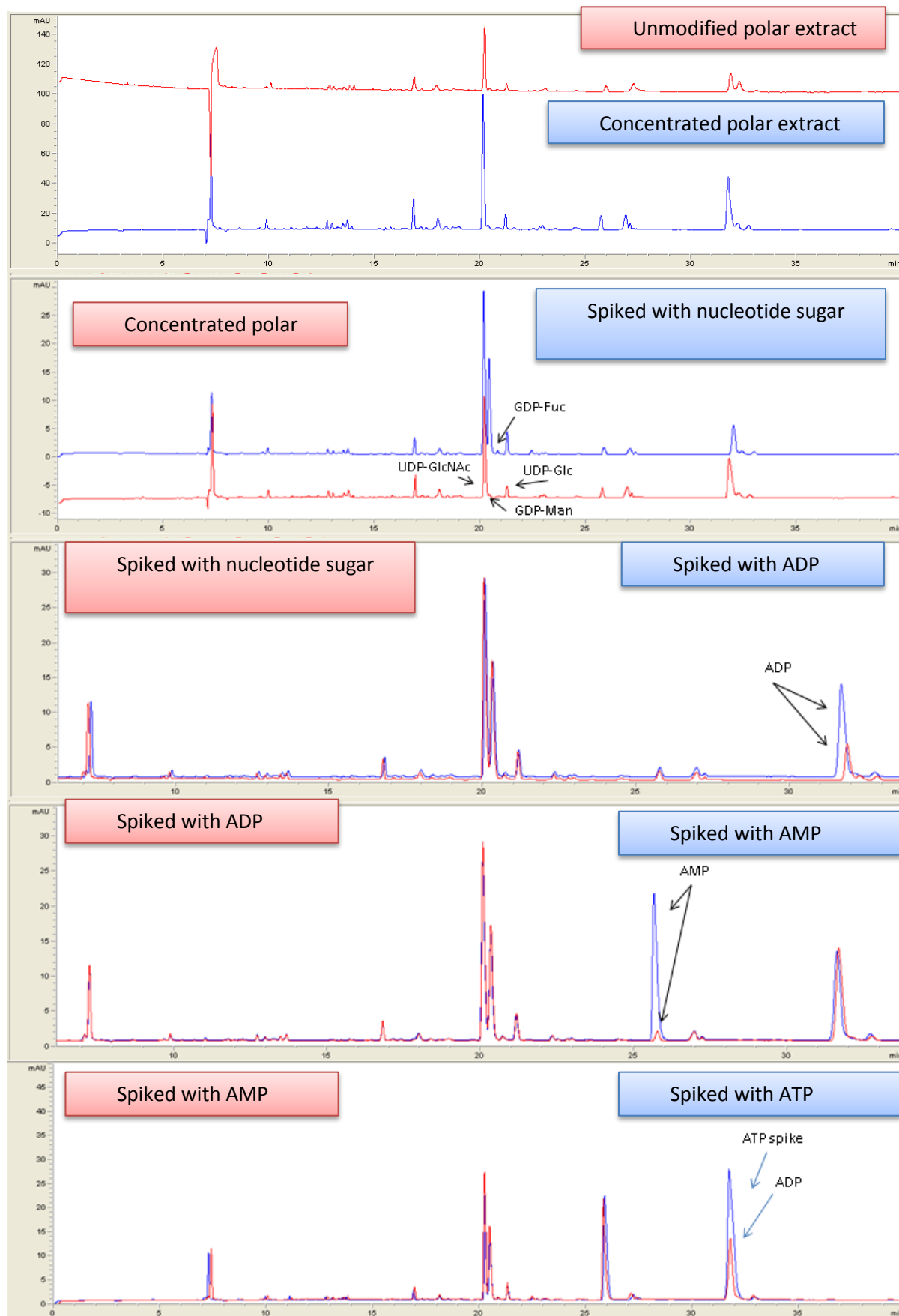


Figure IV. Sample preparation procedure following extraction.

Table I. Relative abundance calculations for each analysed nucleotide sugar in each culture flask.

Carbon Source	Biological Replicate	Day 1 Relative abundance			Day 2 Relative abundance			Day 3 Relative abundance			Day 4 Relative abundance		
		UDP-GlcNAc	GDP-Man	UDP-Glc	UDP-GlcNAc	GDP-Man	UDP-Glc	UDP-GlcNAc	GDP-Man	UDP-Glc	UDP-GlcNAc	GDP-Man	UDP-Glc
Glucose	1	77.77	6.15	16.08	80.78	3.26	15.96	82.59	3.84	13.58	86.92	2.89	10.18
	2	79.61	5.26	15.13	83.70	3.14	13.16	84.90	2.36	12.74	88.51	1.75	9.74
	3	81.12	5.11	13.78	82.25	3.17	14.58	81.48	4.09	14.43	87.45	2.84	9.71
Average		79.50	5.50	15.00	82.24	3.19	14.57	82.99	3.43	13.58	87.63	2.49	9.88
Standard Error		0.97	0.33	0.67	0.84	0.04	0.81	1.01	0.54	0.49	0.47	0.37	0.15
Lactose	1	79.22	2.49	18.29	78.15	3.18	18.67	71.45	5.63	22.93	69.41	4.94	25.64
	2	76.04	3.69	20.27	76.39	4.60	19.01	72.46	3.62	23.92	68.80	6.69	24.51
	3	78.21	3.82	17.96	75.79	3.62	20.59	70.72	5.17	24.12	69.99	6.41	23.60
Average		77.82	3.33	18.84	76.78	3.80	19.42	71.54	4.80	23.66	69.40	6.01	24.58
Standard Error		0.94	0.42	0.72	0.71	0.42	0.59	0.50	0.61	0.37	0.34	0.54	0.59

Table II. Migration time for each analysed nucleotide sugar in each culture flask. * denotes concentrated samples and therefore modified migration times.



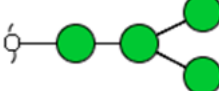


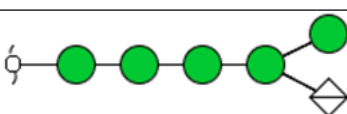
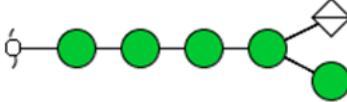

Carbon Source	Biological Replicate	Day 1 migration time*			Day 2 migration time (L*)			Day 3 migration time*			Day 4 migration time (L*)		
		UDP-GlcNAc	GDP-Man	UDP-Glc	UDP-GlcNAc	GDP-Man	UDP-Glc	UDP-GlcNAc	GDP-Man	UDP-Glc	UDP-GlcNAc	GDP-Man	UDP-Glc
Glucose	1	20.54	20.79	21.57	18.92	19.15	19.89	20.41	20.67	21.48	20.64	20.90	21.71
	2	21.23	21.50	22.29	19.27	19.50	20.27	20.35	20.62	21.43	20.22	20.48	21.27
	3	20.08	20.62	21.40	19.01	19.23	19.98	20.43	20.69	21.49	20.49	20.76	21.21
Average		20.61	20.97	21.76	19.07	19.29	20.04	20.39	20.66	21.47	20.45	20.71	21.40
Standard deviation		0.58	0.46	0.47	0.18	0.19	0.20	0.04	0.04	0.04	0.21	0.21	0.27
Lactose	1	19.80	20.02	20.63	19.86	20.08	20.84	19.96	20.19	20.95	20.79	21.04	21.86
	2	20.28	20.51	21.21	19.90	20.13	20.89	20.20	20.43	21.22	19.08	19.30	20.04
	3	22.12	22.41	23.34	21.34	21.60	22.43	20.03	20.26	21.03	18.92	19.14	19.87
Average		20.73	21.46	21.73	20.36	20.61	21.39	20.06	20.29	21.07	19.59	19.83	20.59
Standard deviation		1.23	1.26	1.43	0.84	0.86	0.90	0.12	0.13	0.14	1.04	1.06	1.10

7.3 N-glycan and O-glycan MS/MS structures table

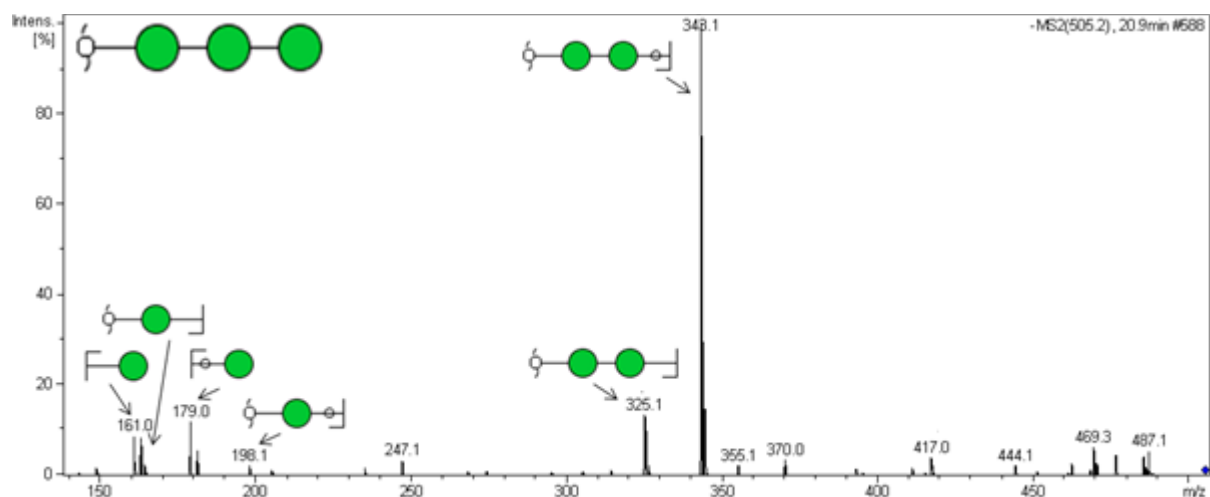
Table III. Refined MS data of N-glycans utilising MS² to determine composition.

SI-No	m/z [M-2H] ²⁻	Composition			RT ± 0.2	Likely structure/s	D2G Rel. % ± S.E	D4G Rel. % ± S.E	D2L Rel. % ± S.E	D4L Rel. % ± S.E
		Hex	HexNAc	Ph _o /Su.						
1	779.3	7	2	0	38.1		0.0 ± 0	0.0 ± 0	1.5 ± 0.3	0.3 ± 0.2
2					39.3		4.3 ± 0.8	2.9 ± 0.6	1.9 ± 0.2	1.8 ± 1.1
3					43.0		1.2 ± 0.1	1.1 ± 0.4	1.8 ± 0.1	1.7 ± 0.2
4	860.3	8	2	0	43.0		40.3 ± 3.5	0.0 ± 0	55.5 ± 1.7	41.0 ± 11.1
5	900.3	8	2	1	34.8		0.0 ± 0	36.6 ± 6.6	0.4 ± 0.0	0.0 ± 0
6					36.8		1.9 ± 0.3	1.6 ± 0.3	0.8 ± 0.1	0.9 ± 0.1
7					39.6		0.9 ± 0.3	3.2 ± 0.2	1.6 ± 0.2	2.4 ± 0.8
8	941.3	9	2	0	40.2		8.4 ± 1.4	13.2 ± 2.5	14.2 ± 1.0	18.1 ± 3.9
9					44.1		3.2 ± 0.2	2.3 ± 0.2	3.0 ± 0.4	0.0 ± 0
10	981.3	9	2	1	35.0		2.1 ± 0.1	1.8 ± 0.9	0.0 ± 0	0.0 ± 0
11					40.9		13.9 ± 1.1	16.8 ± 3.4	8.9 ± 1.0	13.1 ± 1.3
12	1022.4	10	2	0	40.8		3.1 ± 0.9	7.3 ± 2.3	4.1 ± 0.4	7.8 ± 2.8
13					41.3		0.4 ± 0.2	0.0 ± 0	0.0 ± 0	0.0 ± 0
14					43.5		0.3 ± 0.2	0.0 ± 0	0.3 ± 0.2	0.0 ± 0
15	1062.9	10	2	1	36.9		13.7 ± 2.3	7.8 ± 3.9	4.8 ± 0.9	11.1 ± 3.8
16					41.6		0.00 ± 0	1.3 ± 0.7	0.0 ± 0	0.0 ± 0
17					42.2		2.1 ± 0.3	0.0 ± 0	0.0 ± 0	0.0 ± 0
18	1103.9	11	2	0	44.1		0.9 ± 0.5	1.0 ± 0.0	0.3 ± 0.2	0.7 ± 0.1
19					45.7		0.8 ± 0.1	1.0 ± 0.2	0.6 ± 0.1	0.0 ± 0
20	1143.9	11	2	1	37.7		2.6 ± 0.4	2.4 ± 0.6	0.4 ± 0.1	1.2 ± 0.4

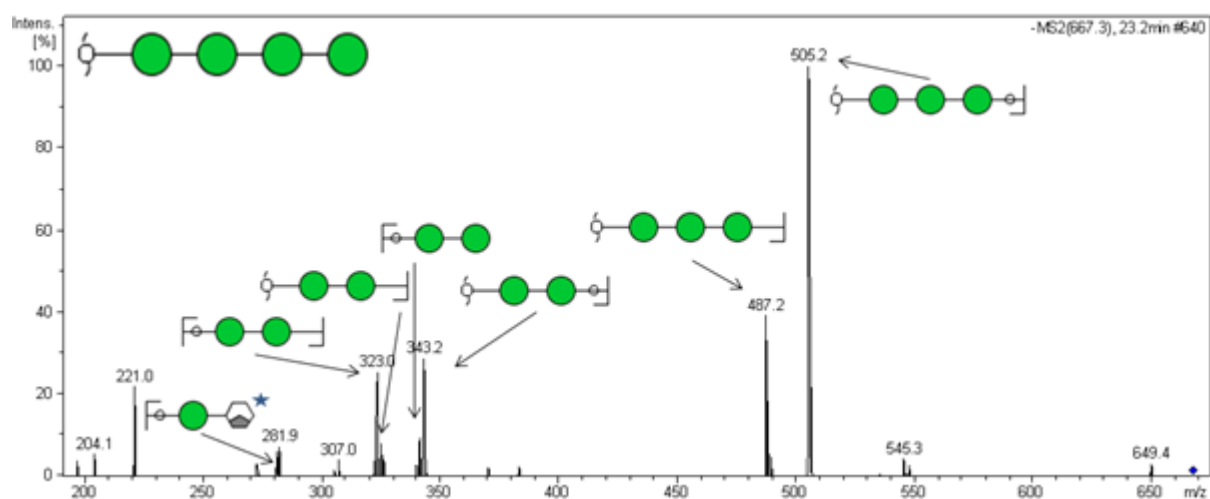
Table IV. Refined MS data of *O*-glycans utilising MS² to determine composition and number of antennae.

SI-No	m/z [M-H] ⁺	Composition		R.T ± 0.2	Likely structure/s	D2G Rel. % ± S.E	D4G Rel. % ± S.E	D2L Rel. % ± S.E	D4L Rel. % ± S.E
		Hex	HexA						
1	505.2	3	0	20.9		3.3 ± 2.0	5.3 ± 0.5	3.3 ± 0.6	7.8 ± 2.6
2	667.2	4	0	23.1		11.7 ± 1.9	23.9 ± 2.8	31.9 ± 4.9	15.8 ± 6.3
3				24.5		27.7 ± 1.6	20.7 ± 2.9	15.7 ± 7.9	48.0 ± 3.2
4	829.3	5	0	26.0		32.5 ± 8.6	14.2 ± 6.4	36.3 ± 3.2	20.3 ± 0.4
5	843.3	4	1	23.4		19.9 ± 9.7	32.2 ± 7.1	6.9 ± 2.8	8.1 ± 0.1
6	1005.3	5	1	23.1		1.9 ± 0.3	1.5 ± 0.4	3.9 ± 1.6	0.0 ± 0.0
7				24.7		3.0 ± 0.5	1.1 ± 0.2	1.9 ± 0.3	0.0 ± 0.0
8				25.6		0.0 ± 0.0	1.1 ± 0.8	0.0 ± 0.0	0.0 ± 0.0

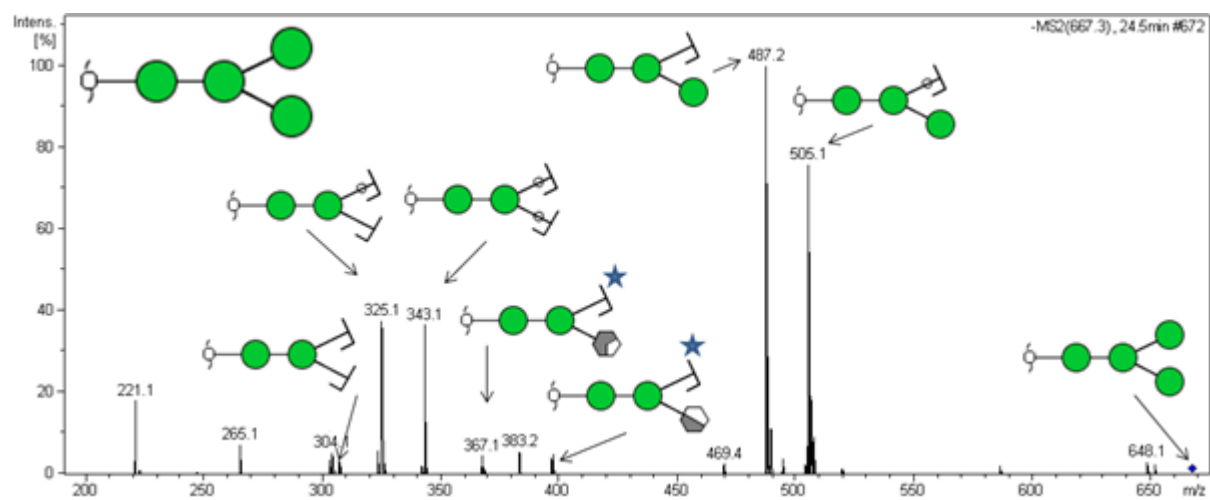
7.4 Annotated MS/MS of O-glycans



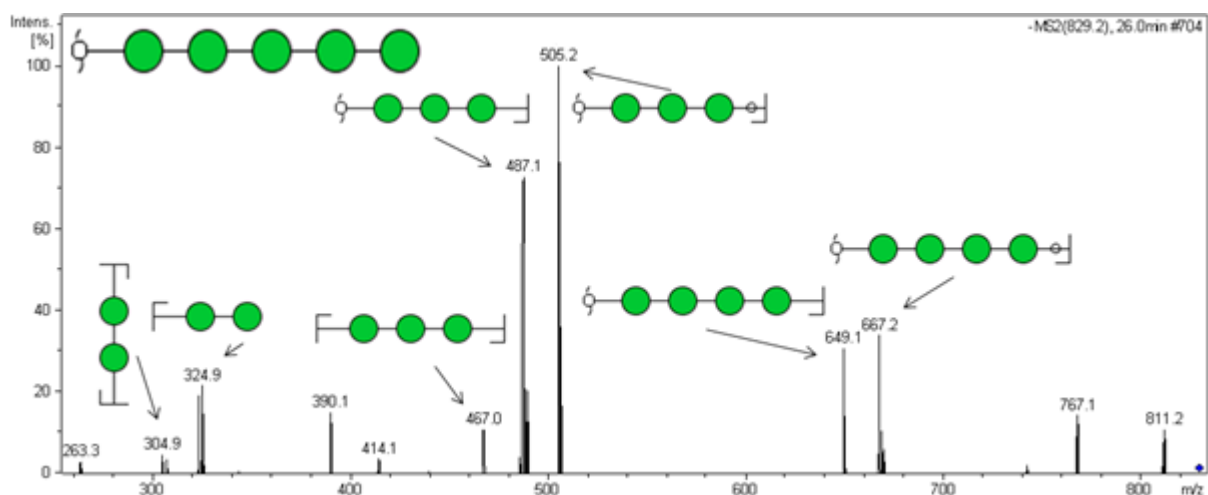
505.2 m/z with retention time of 20.9 minutes



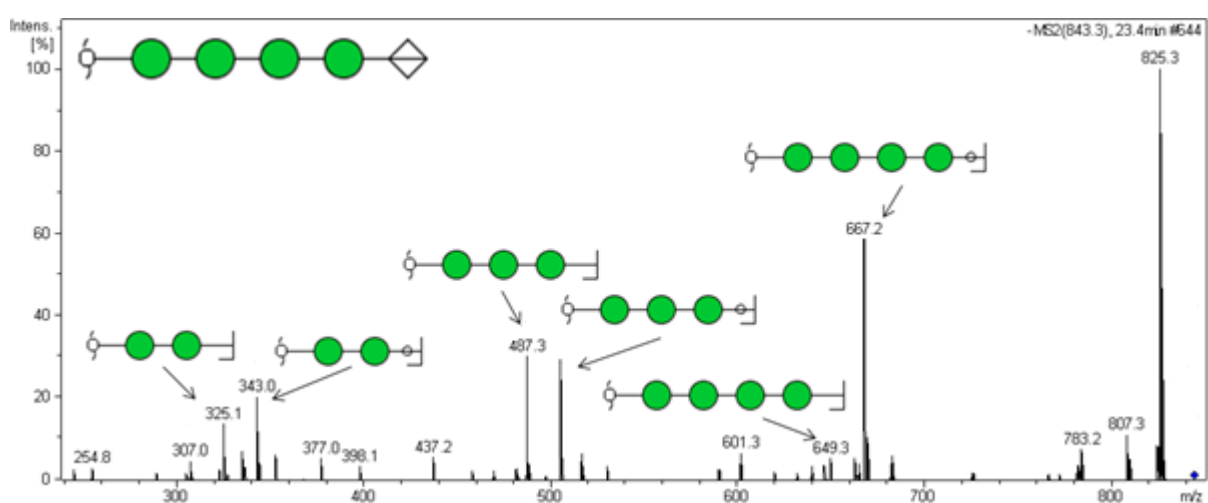
667.2 m/z with retention time of 23.2 minutes



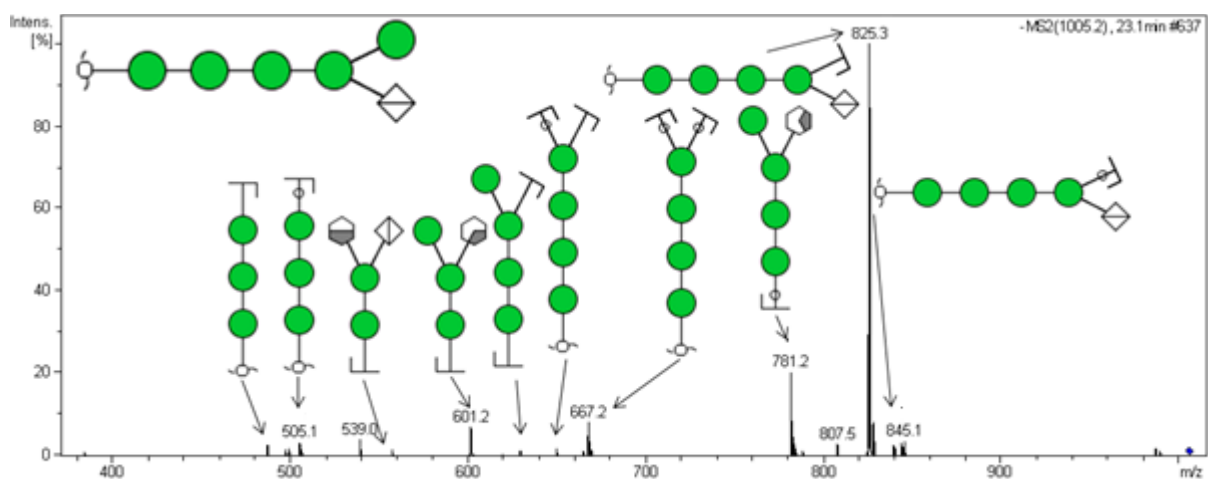
667.2 m/z with retention time of 24.5 minutes



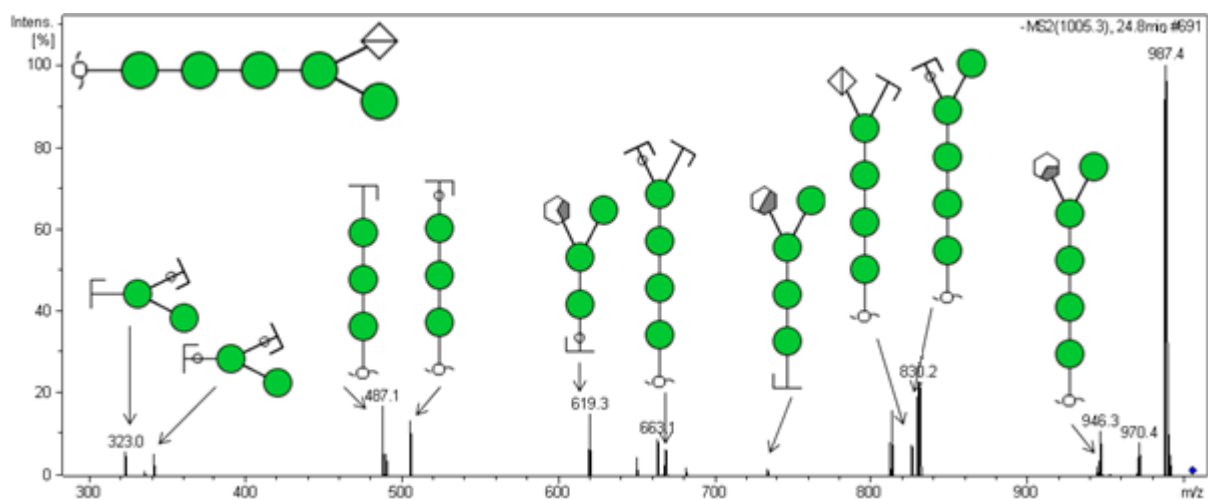
829.2 m/z with retention time of 26.0 minutes



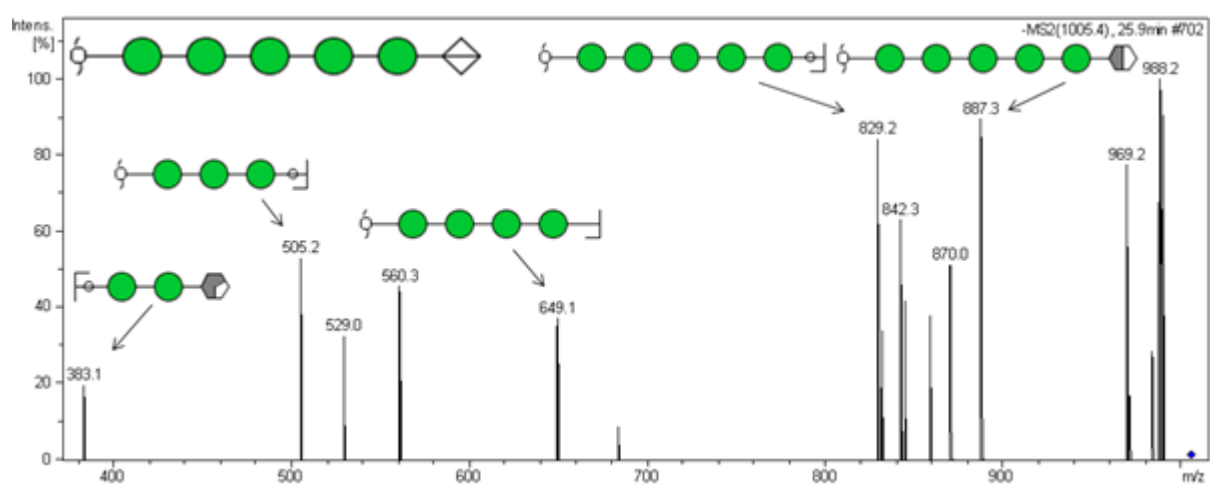
843.3 m/z with retention time of 23.4 minutes



1005.3 m/z with retention time of 23.1 minutes



1005.3 m/z with retention time of 24.8 minutes



1005.3 m/z with retention time of 25.9 minutes

7.5 Identification of CBHI as a major constituent of total secreted protein

SDS-PAGE Gel

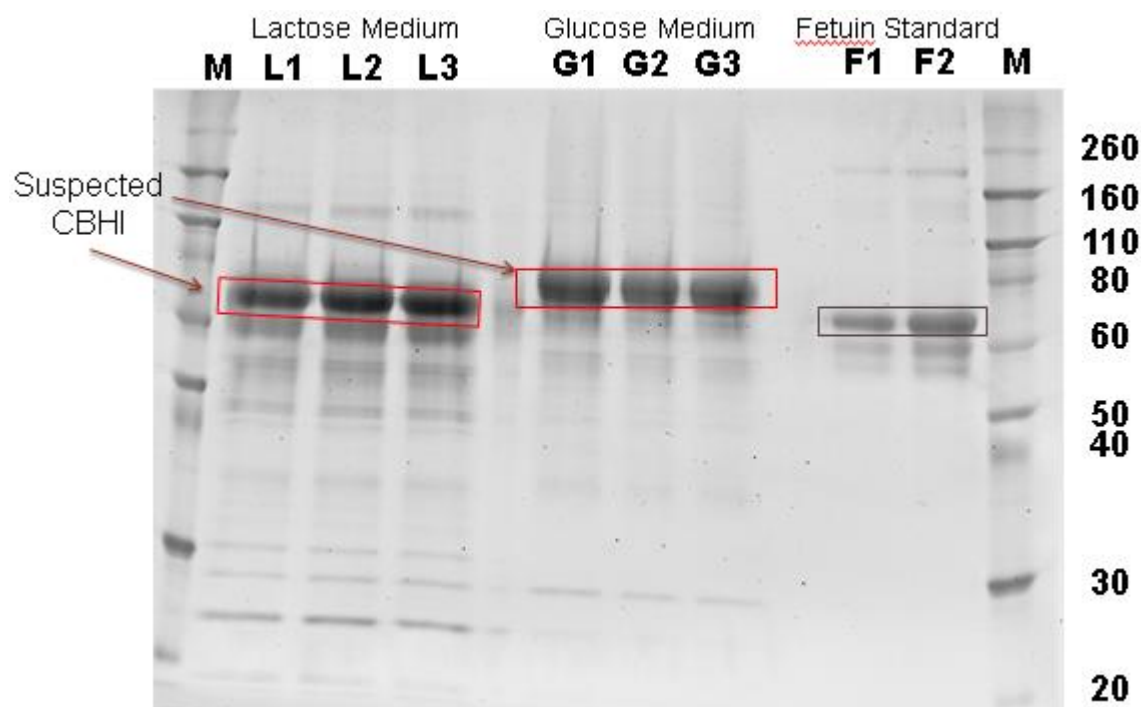


Figure V. 10% Tris-glycine gel analysing secreted protein from culture supernatant on day 4.

Proteome Discoverer search parameters

- Spectrum selection:
 - Precursor selection: Use MS1 Precursor
 - Use new precursor re-evaluation: True
 - Lowest charge state: 2
 - Highest charge state: 8
 - Min/max precursor: 350-1750 Da
 - Minimum peak count: 5
 - ESI ionisation, positive mode, HCD fragmentation
 - Signal to noise threshold: 1.5
- Mascot properties:
 - Database: SwissProt
 - Maximum missed cleavage sites: 2
 - Taxonomy: Fungi
 - Peptide cut off score: 10
 - Peptide without protein count off score: 5
 - Mudpit scoring: Automatic
 - Protein relevance threshold: 20
 - Protein relevance factor: 1

- Precursor mass tolerance: 10 ppm
- Fragment mass tolerance: 0.05 Da
- Dynamic modifications:
 - Oxidation (M)
 - Acetyl (*N*-term)
 - Deamidated (N)
 - Gln -> pyro-Glu (*N*-term Q)
 - Glu -> pyro-Glu (*N*-term E)
- Static modifications:
 - Carbamidomethyl (C)
- Peptide validator:
 - Search against decoy database: True
 - Target false discovery rate (Strict): 0.01
 - Target false discovery rate (Relaxed): 0.05

Protein identification of gel bands

Table V. Proteome discoverer results of analysed gel bands from figure V.

Carbon source	Accession	Description	Average Coverage	Avg. # of prot.	Avg. # of unique peptides	Avg. # of different peptides	Avg # of PSM's
Glucose	P62694	Exoglucanase 1 (CBH1)	9.94%	22	5	6	776
	B8N717	Probable α-L-Arabinofuranosidase B	1.38%	2	1	1	1
	P07987	Exoglucanase 2 (CBH2)	6.58%	1	2	4	4
	P07981	Endoglucanase 1 (EGL1)	5.88%	1	1	1	5
	P07982	Endoglucanase 2 (EGL2)	1.44%	1	1	1	3
Lactose	P62694	Exoglucanase 1 (CBH1)	9.94%	22	6	6	1101
	B8N717	Probable α-L-Arabinofuranosidase B	2.77%	2	1	2	6
	P07987	Exoglucanase 2 (cbh2)	9.13%	1	5	5	222
	Q7Z9M8	Xyloglucanase	12.17%	1	7	11	50
	P07987	Endoglucanase EGL1	5.88%	1	2	2	25